Optimal Planning and Economic Dispatch of Community Microgrids

Junyuan Zhao, Department of Electrical & Computer Engineering
McGill University, Montreal

September, 2020

A thesis submitted to McGill University in partial fulfillment of the requirements of the degree of

Master of Science

Abstract

With the increasing penetration of renewable energy and other distributed energy resource (DER) systems in distribution networks, the concept of community microgrids has become a desirable option for power system planners. Community microgrids can operate either connected with the centralized grid or isolated, with the benefit of maintaining supply during main grid disturbances, as well as allowing coordinated local control of DERs with and without the support of the main grid. Some components, which are more and more employed in the microgrids such as combined heat and power (CHP) units and electric vehicle charging stations (EVCS), also need to be considered in the planning and operation stages of microgrids, especially the impact of fast charging facilities (FCF) in the community, which entails significant demand fluctuations and high demand peaks.

In this thesis, components of a typical community microgrid are modeled. An optimal microgrid asset planning approach is introduced and validated on different scenarios, and parameters whose fluctuation may affect the costs are explored in sensitivity analysis. The input data especially the electrical load data are analyzed, and EVCSs are integrated into microgrid planning processes. As an efficient way to improve energy utilization, demand response is considered in the grid-connected mode of the community microgrid. The work further investigates microgrid economic dispatch based on a decision tree regressor. The decision tree is prevented from overfitting by post pruning, and the multi-output decision tree is used to improve the overall outcome in terms of operational cost performance.

Abrégé

Avec la pénétration croissante des énergies renouvelables et d'autres systèmes de ressources énergétiques distribuées (DER) dans les réseaux de distribution électrique, le concept des microréseaux communautaires est devenu une option souhaitable pour les planificateurs de ces systèmes. Un microréseau communautaire peut fonctionner soit connecté au réseau principal, soit îloté, avec l'avantage de renforcer la fiabilité du service en pouvant maintenir les approvisionnements en cas de panne du côté du réseau principal, ainsi que de pouvoir coordonner localement la production d'énergie distribuée autant avec que sans l'apport du réseau principal. Certains composants de plus en plus utilisés dans les microréseaux tels que les unités de production combinée de chaleur et d'électricité (CHP) et les bornes de recharge pour véhicules électriques (EVCS) doivent également être pris en compte dans les étapes de planification et d'exploitation, en particulier l'impact des installations de charge rapide (FCF) dans la communauté, qui peut connaître des fluctuations importantes et des pics de charge élevés.

Dans cette thèse, les composants des microréseaux communautaires sont modélisés. Une approche de planification des actifs optimale est introduite et validée sur différents scénarios, et les paramètres dont la fluctuation peut affecter les coûts sont explorés par des analyses de sensibilité. Les données d'entrée, en particulier les données de charge électrique, sont analysées et les EVCS sont intégrés dans le processus de plannification d'un microréseau. En tant que moyen efficace d'améliorer l'utilisation de l'énergie, le pilotage de charge est considéré dans le mode connecté au réseau principal du microréseau

communautaire. Ensuite, le travail a, en outre, étudié la répartition économique sur la base d'u régresseur de lpararbre de décision. On se soucie du fait que l'arbre de décision soit en mesure de bien effectuer la répartition économique même lorsque confronté à de nouvelles conditions d'exploitation, et l'arbre de décision multi-sortie est utilisé pour améliorer le résultat global.

Acknowledgements

I would like to thank my supervisor Prof. François Bouffard for his support throughout my master's studies. I am very grateful for the opportunities he offered me. He guided me with his insights and inspirations, as well as his continuous efforts to introduce me to microgrid systems. I learnt a lot from discussions with him and his courses. I also acknowledge the financial support received from InnovÉÉ, OPAL-RT and the NSERC.

Furthermore, I appreciate my friends in the power lab. I will always remember their help and encouragement. And many thanks to my roommate. I also appreciate my friends in China. Special thanks and love to my boyfriend. It is a miracle to meet him.

Finally, I would like to express my deepest love and gratitude to my parents who support me with their unparalleled love and understanding. I can never thank them enough for the possibility that I can become the person I want to be.

Contribution of Authors

My contributions can be summarized as follows:

In Chapter 1, a literature review on the background of community microgrids is conducted, and challenges on the asset sizing and economic dispatch problems are explained. In Chapter 2, modeling of the main components in typical community microgrids is introduced, which is widely adopted in existing research works. In Chapter 3, input data of the asset sizing problem are analyzed and the impact of EVCSs on community microgrids is outlined. Chapter 4 applies a microgrid asset sizing method on a community microgrid, and several case studies together with a sensitivity analysis are done. In Chapter 5, a decision-tree-based economic dispatch algorithm is designed and applied on a community microgrid. Chapter 6 summarizes the major work of the thesis and proposes recommendations for future work.

My supervisor François Bouffard has participated in the whole process of the thesis work. He has suggested the research direction and made throughout revisions to the thesis. Work performed in Chapter 4 is based on the optimization algorithm brought up by Quashie et al (2018). The load data is also provided by Mike Quashie. The coding work in Chapter 4 is done in collaboration with fellow graduate student Anindita Golder. She has been consulted on the optimization problem construction and debugging. Anand et al (2020) and Prof. Rajapakse at University of Manitoba has provided data of electric vehicle charging stations.

Table of Contents

Abstract i

Abrégé ii

Acknowledgements iv

Contribution of Authors v

List of Figures x

List of Tables xi

1 Introduction **1**

1.1 Background 1

1.2 Challenges with Asset Sizing and Economic Dispatch of Community Microgrids 3

1.3 Problem Identification 4

1.3.1 Thesis Statement 4

1.3.2 Research Objectives 4

1.3.3 Methodology and Research Tools 5

1.4 Contributions 6

1.5 Thesis Outline 6

2 Community Microgrid System Description **8**

2.1 Diesel Generator 9

2.2 Combined Heat and Power (CHP) Units 10

2.3 Wind Turbine 11

2.4 Photovoltaic (PV) Systems . . . 14
2.5 Energy Storage Systems (ESS) . . . 14
2.6 Electric Vehicle Charging Stations in Community Microgrids . . . 16
2.6.1 Literature Review . . . 16
2.6.2 Modeling of EV Parking Behaviors and Charging Demands . . . 17
2.6.3 Consideration on the EVCSs in a Community Microgrid . . . 18
2.7 Demand Response in a Community Microgrid . . . 19
2.8 Chapter Summary . . . 21

3 Asset Sizing Data Requirements and Analysis 22
3.1 Electrical Load Data . . . 23
3.2 Net Load Data . . . 25
3.2.1 Demand-Wind-PV Data . . . 25
3.2.2 Demand-PV Data . . . 29
3.3 EVCS Data . . . 33
3.4 Chapter Summary . . . 34

4 Community Microgrid Asset Sizing 36
4.1 Introduction . . . 36
4.2 Community Microgrid Asset Sizing Formulation . . . 37
4.3 Asset Sizing Results and Discussion . . . 39
4.3.1 Case I (Baseline): Diesel, Wind and ESS . . . 40
4.3.2 Case II: Diesel, Wind, ESS and PV . . . 41
4.3.3 Case III: Diesel, Wind, ESS, PV and CHP . . . 42
4.3.4 Case IV: Diesel, Wind, PV and CHP . . . 43
4.3.5 Case V: Diesel, Wind, ESS, PV, CHP and DR . . . 43
4.3.6 Case VI: Grid-connected; Diesel, Wind, ESS, PV, CHP and DR . . . 44
4.3.7 Adding EVCSs . . . 45
4.4 Sensitivity Analysis . . . 46

4.4.1 Overview of Sensitivity Analysis 46
4.4.2 Implementation of the Sensitivity Analysis 47
4.5 Chapter Summary 48

5 Implementing Community Microgrid Economic Dispatch with a Decision-Tree-Based EMS 50
5.1 Overview 50
5.2 Decision-Tree-Based EMS Data Analysis 52
5.3 Decision Tree Algorithm Outline 53
5.4 Decision Tree Design and Calculation 55
5.4.1 Training and Pruning of Decision Trees 55
5.4.2 Improving the Results with a Multi-Output Decision Tree 56
5.5 Evaluation of the Decision-Tree-Based EMS Against Fully-Optimized Economic Dispatch 59
5.6 Chapter Summary 61

6 Summary and Future Work 62
6.1 Summary 62
6.2 Recommendations for Future Work 64

List of Figures

1.1 Community Microgrid . . . 2

2.1 CHP System Components and Operation. . . . 10
2.2 Weibull Distribution Function. . . . 12
2.3 Wind Power Curve. . . . 13

3.1 Optimal k Value for Electrical Load. . . . 25
3.2 Clusters of Demand (k=3). . . . 26
3.3 Clusters of Demand (k=2). . . . 27
3.4 Data Plotting of Demand-Wind-PV. . . . 28
3.5 Data Plotting of Wind Generation. . . . 29
3.6 3D Data Plotting of Demand-Wind-PV. . . . 30
3.7 Elbow Method for the Demand-Wind-PV Data. . . . 31
3.8 Elbow Method for the Demand-PV Data. . . . 32
3.9 EVCS Annual Charging Demand. . . . 33
3.10 Daily Demand With and Without EVCS. . . . 34

5.1 Generation of a Decision Tree. . . . 53
5.2 Total Impurity Versus $alpha$. . . . 56
5.3 Number of Nodes and Depth Versus $alpha$. . . . 57
5.4 Accuracy Versus $alpha$. . . . 58
5.5 Decision Tree Before Pruning. . . . 58
5.6 Decision Tree After Pruning. . . . 59

5.7 Multi-output Decision Tree for Energy Storage and Diesel Generation. . . . 59

List of Tables

3.1 Silhouette Scores 23
3.2 Silhouette Scores 28
3.3 Silhouette Scores 30
3.4 Silhouette Scores 31

4.1 Capital Costs and Maintenance Costs 40
4.2 Rating of Each Resource in Case I 41
4.3 Investment and Operation Costs for Case I 41
4.4 Rating of Each Resource in Case II 41
4.5 Investment and Operation Costs for Case II 41
4.6 Rating of Each Resource in Case III 42
4.7 Investment and Operation Costs for Case III 42
4.8 Rating of Each Resource in Case V 43
4.9 Investment and Operation Costs for Case V 43
4.10 Rating of Each Resource in Case VI 44
4.11 Investment and Operation Costs for Case VI 44
4.12 Rating of Each Resource Adding EVCSs 45
4.13 Investment and Operation Costs adding EVCSs 45
4.14 Sensitivity Analysis 48

5.1 MSE Score of Single Outputs 58

Chapter 1

Introduction

1.1 Background

Community microgrids are playing a more and more important role in modern power grids. Villages, remote communities, islands and municipal distribution utilities connected to larger grids are regarding microgrids as an approach to increasing energy independence and supply resilience and decreasing emissions. More possibilities in the electricity market can also be explored. For instance, the Brooklyn Microgrid [1] is a successful example in which residential and commercial solar panel owners can sell solar energy to other residents in New York City, so as to reduce pollution and benefit the local economy. Microgrids can also reduce long-distance transmission losses and would be a desired option for remote communities. For the time being, more than 1.3 billion people in the world do not have access to modern grids, in which 631 million are from the area of Sub-Saharan Africa [2]. In Nigeria, 60% of the citizen do not have supply from the national grid [2]. Sustainable community microgrids have great potential in these areas.

Distributed energy resources (DERs) are widely seen in community microgrids. DERs include PV generation, small wind generation, small hydro, energy storage systems, demand response, electric vehicles, smart buildings, etc. Among the main DER technologies, PV and storage have the most fast growth. The annual growth rate of PV capacity

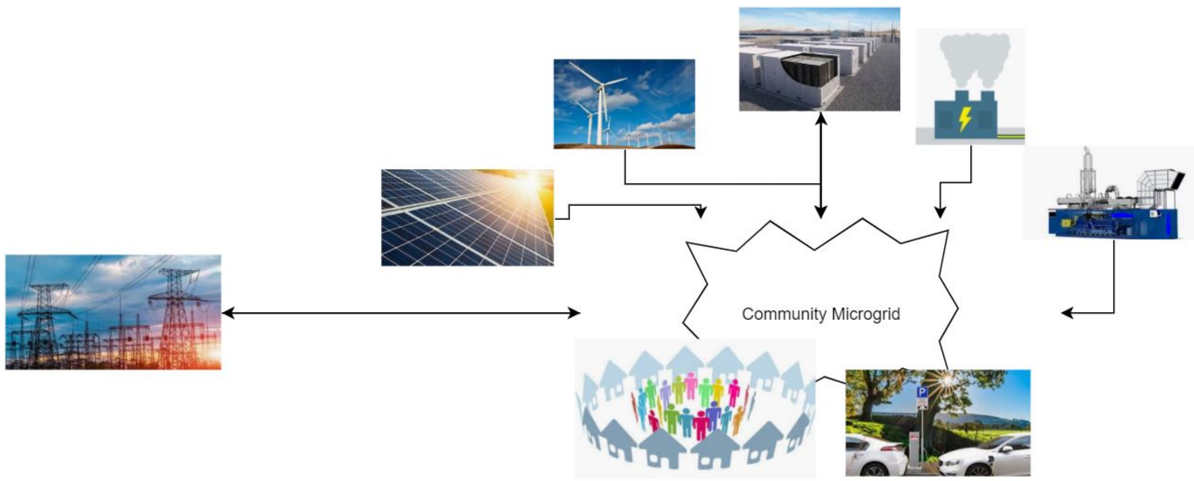

Figure 1.1: Community Microgrid

is over 25% during the last five years [3]. More that 486 GW PV generation is installed in the world. In 2018, a new installation of PV is 94 GW globally, among which Asia is over 70%. China installed 44GW of PV in 2018, with an increase of 34% [3]. Wind installation follows a similar trend. The Global Wind Energy Council published that over 60 GW of wind generation was installed in 2019 worldwide, with an 18% percent increase compared with 2018 [4].

The benefits of DERs include resilience during power outages or other instability, reduction of carbon footprint and decrease of energy costs. DERs generate AC/DC power with various frequencies, and the generated power is converted to the same frequency as the power system. The AC power with diverse frequency is converted to DC and then synchronized with the power system by power electronic converters, namely inverters. Inverters thus serve as the interaction between the DERs and the grid and is sometimes combined with the functions of ancillary services and disturbance protection [5].

1.2 Challenges with Asset Sizing and Economic Dispatch of Community Microgrids

Community microgrids can integrate distributed generation (DG) units and energy storage systems (ESS) so as to achieve energy savings and decrease greenhouse gas emissions. However, it is challenging to do the optimal sizing and economic dispatch of the microgrids due to the randomness of the DG generation from wind and solar units.

Renewable generation such as wind and solar generation can be intermittent and unpredictable, which will not only bring challenges to the quality of energy supply and safety of the microgrid, but also require better ways to satisfy continously the power balance. Since the renewable energy resources fluctuate greatly with weather parameters such as wind and solar irradiation, dispatchable energy resources in the microgrids need to supplement these fluctuations.

The problem becomes more complicated when more random and fluctuating loads such as electric vehicle charging stations (EVCSs) are integrated. Fully-electric EVs are one of the focuses in the EV industry. As a result, battery capacities are continuously being enlarged. To ensure reasonable charging times, EVs with large recharging power are more and more common. Manufacturers like Tesla are already adopting 11 kW and 16.5 kW chargers. Moreover, considering the situation in most commercial and working areas where many EVs could be charging simultaneously in EVCSs, the power characteristics of the EVCSs have to be investigated more fully. Many papers such as [6] have not considered the ability of community microgrids to withstand the fluctuation brought by significant numbers of EVCSs. These challenges must be considered in the long-term planning stage and microgrid economic dispatch, so that proper combinations and sizes of diverse energy sources can be chosen, and strategic deployment of energy storage systems and demand response technologies can also be included.

As an important characteristic of many community microgrids, multi-energy-flows (electricity, heat, gas, etc.) are a common place and need to be considered as a whole. Not only the electric power balance, but also the heat load and generation should be included in the planning and operation of the microgrid.

In this thesis, the above challenges are considered in asset sizing and economic operation. There are also other problems affecting community microgrids regarding the market, security, regulations and laws; these can be explored in future work.

1.3 Problem Identification

1.3.1 Thesis Statement

In this thesis, components in community microgrids are introduced, including diesel generators, combined heat and power (CHP) units, wind and PV generation and ESS. Characteristics of the charging and discharging of EVCSs are studied and integrated into the design of the microgrid. Constraints for demand response (DR) are also considered in the modeling. The sizing problem formulation is then illustrated, and the model is run on several case studies. The outputs of the sizing problem are then set as the inputs of an economic dispatch problem. In order to allow for in-field programmable logic controller implementation, the economic dispatch is mapped to a decision tree regressor, and the results are improved by post-pruning to prevent overfitting. A multi-output decision tree is also used to boost the economic dispatch results.

1.3.2 Research Objectives

This thesis is focused on asset sizing and economic dispatch of community microgrids, while considering the challenges introduced before. The objectives of this thesis consist of three aspects and are achieved as follows:

Firstly, a community microgrid model including multiple DGs, ESS, DR and EVCSs is built to investigate the influence of these components to microgrids and their relationships. Wind and PV generations are renewable generations in the microgrid, which relies on an ESSs to address the problem brought by the intermittent and variable nature. CHP units provide heat and electricity simultaneously, and diesel generators are also prepared in the system, and demand response serves as another type of distributed energy resource. The ability of community microgrids to meet the demand of EV charging is investigated. Since power system failures are not discussed within the thesis work, the main grid is simplified as a constant in this thesis.

Secondly, a community microgrid asset sizing scheme is proposed. The sizing takes the annual investment and operational costs as the minimization objective, and consideres the constraints of all the components introduced before. Before different scenarios are studied, the input data are analyzed with the clustering method to structure a number of typical operating scenarios. Several case studies are carried out to investigate the influence of the essential components within the microgrid. A sensitivity analysis is also conducted to investigate futher the influence of the system parameters.

Thirdly, with the objective of creating a practical rule-based energy management system (EMS) for the microgrid, a machine-learning-based economic dispatch method is proposed and validated. A regression tree approach is used, and post-pruning is applied. We demonstrate that the proposed EMS provides comparably good results when compared to a fully-optimized economic dispatch problem.

1.3.3 Methodology and Research Tools

In this thesis, the community microgrid asset sizing problem is formulated as a linear programming problem. This is carried out through theoretical methodology and model-based optimization. Numerical experiments are carried out using a commercial algebraic modelling tool (GAMS [7]) and a commercial mixed-integer linear programming solver (CPLEX [8]).

Machine learning methods of data clustering is used in the pre-processing of the input data (load, PV, wind and EV charging), and several scenarios are compared to investigate the influence and relationships of the components in the microgrid. Once asset sizes are determined, an energy management system (EMS) is designed for the microgrid. In the context of this thesis, the EMS consists of an economic dispatch algorithm. As the EMS is targeted for implementation in the field in a programmable logic controller, a rule-based economic dispatch algorithm has to be designed. A systematic way to obtain such a rule base is to train a regression tree based on the input-output relationship of a large number of fully-optimized economic dispatch runs. The Scikit-learn library in Python is used, and methods such as post-pruning and multi-output regression tree are also adopted to improve economic dispatch accuracy.

1.4 Contributions

The contributions of this thesis can be summarized as follows:

1. The mathematical models of the generation and load in community microgrids are introduced, and the important parameters related to the sizing and economic problems are explained. Characteristics of the important inputs such as EVCS charging/discharging and electrical loads are presented. Such analysis is the foundation of the understanding of the community sizing and economic dispatch problems.

2. A microgrid asset sizing method is proposed for community microgrids. The impacts of the components to the microgrid are explored. The parameters in the sizing problem are also studied.

3. A decision-tree-based economic dispatch algorithm is proposed and validated. Approaches to improve the algorithm accuracy are used.

1.5 Thesis Outline

The remainder of the thesis is structured as follows:

Chapter 2 presents a community microgrid system description, including modeling of diesel generators, combined heat and power units, wind and PV generation and energy storage systems. The characteristics of these components provide a basic understanding of the system. Also, the integration of electric vehicle charging stations are investigated, and demand response is introduced. Community microgrids are usually connected with the main grid, but can also operate in the island mode when the main grid is down.

Chapter 3 presents data requirements of the sizing problem. The data to be used in a community microgrid sizing are analyzed, and for the given case study, the annual time series data rather than the typical day or typical scenario data are finally adopted based on the analysis.

Chapter 4 presents a community microgrid asset sizing method. The optimization problem is introduced and run on several case studies, so as to investigate how the investment and operational costs change when the PV generation, CHP units, demand response and EVCSs are added and when the ESS is removed. The grid-connected mode is also studied. The impacts of each component are illustrated, and a sensitivity analysis is carried out changing the important parameters. The effect of main grid connection is also analyzed when demand response is added.

Chapter 5 proposes a decision-tree-based economic dispatch method as an EMS, which can be implemented in an industrial controller for community microgrids. The decision tree is built and used on the data from the sizing results and is pruned, and the multi-output decision tree is also introduced. The results are compared to the traditional economic dispatch with the optimization method.

Chapter 6 summarizes the main conclusions of this thesis and suggests some future research improvements.

Chapter 2

Community Microgrid System Description

Distributed energy resources include distributed generation (DG), demand response and energy storage systems (ESS). All the energy resources in this thesis can be divided into dispatchable and non-dispatchable units. Dispatchable units include diesel generators, CHP units and non-generating units such as ESS and DR. The intermittent generations in this thesis, i.e. PV and wind generations, are categorized as non-dispatchable units. In this section, the distributed energy resources in the community microgrid are modeled.

As is illustrated in Section 4.3.6, the main grid is simplified as a flat power profile, which is easier to manage, and requires less overcapacity on the main grid side. At the same time, since the microgrid is able to maintain a flat power profile with the grid, its energy expenses are fully predictable and its capacity (i.e., demand) charges are also fully predictable.

2.1 Diesel Generator

Diesel generators can provide a constant power during a period of time. By using a governor, fuel flow rates can be regulated so that the engine speed can be constant, thus maintaining a pre-set operating point.

The mathematical model of a diesel generator is based on its efficiency curve, which describes the relationship between the efficiency at burning fuel and the electrical load on the generator [9]. Then the output of the electrical generator can be generated from the efficiency and the loading of the diesel engine:

$$P_{gen}(y,t) = P_{eng}(y,t)\eta_i^e \tag{2.1}$$

where P_{eng} and P_{gen} are the loads on the engine and the generator, respectively, and y and t represent year and time, respectively. The electrical efficiency is η_i^e, in which e means electricity and i is the numbering if there are multiple generators.

Besides, the output of a diesel generator is restricted by its upper and lower generation limits:

$$0 \leq P_{gen}(y,t) \leq x_i(diesel) \tag{2.2}$$

where $x_i(diesel)$ is the capacity of the diesel generator i.

As for other characteristics, reference [9] gives the electrical generator performance curve and diesel engine performance curve. The fuel consumption can be written as a function of generator loading, and the fuel curve is also given in [9]. These characteristics could provide a better understanding of the generation of diesels. Variable efficiency has a minor impact on asset sizing and economic dispatch because diesel generators tend to operate at close to 100% most times.

2.2 Combined Heat and Power (CHP) Units

CHP systems can provide heat and power at the same time. In CHP plants, the waste heat in power generation is utilized in residential heating systems rather than emitted. CHP generation is an efficient way to improve the efficiency of coal-fired power plants [10]. A CHP system is comprised of several components: a prime mover, an electric generator and a heat recovery unit, as is shown in Figure 2.1 [9]. The prime mover is where the fuel is consumed. Reference [9] introduced several prime movers, such as reciprocating internal combustion engines, combustion turbines, steam turbines, microturbines and fuel cells. Many kinds of fuel sources can be used, and the widely used gas-fired CHP is discussed in this thesis. The recovery unit is where the waste heat generated from the prime mover can be transformed into usable thermal energy [9].

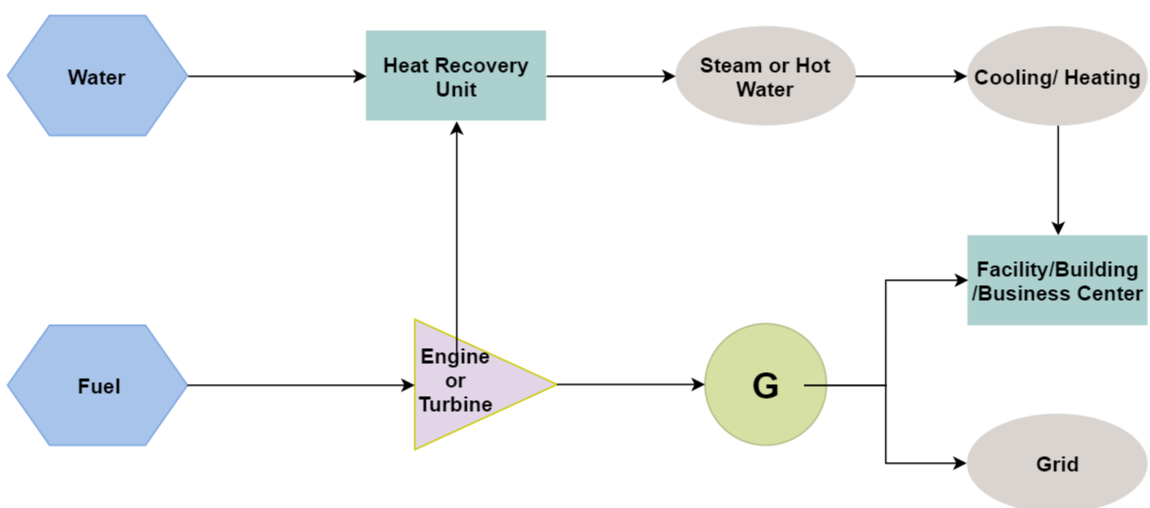

Figure 2.1: CHP System Components and Operation.

The efficiency of a CHP system depends on the energy generation technology, the system design, etc. Since the electricity and heat energies are generated at the same time, there exist many indices to evaluate the efficiency of the system, among which the total system efficiency and the effective electric efficiency are most commonly used [11].

The total system efficiency η_i of a CHP set $i \in I_N$is calculated as below, in which I_N is the set of CHP units and i is the numbering:

$$\eta_i = \frac{P_i^e + P_i^h}{l_i^f} \tag{2.3}$$

where P_e^i and P_h^i are net useful power and thermal outputs, respectively, and l_f^i is the total fuel input. The efficiency η_i is usually provided from manufacturer data.

The effective electric efficiency provides a comparison between CHP systems to conventional power generation. The calculation is in (2.4):

$$\eta_i^e = \frac{P_i^e}{l_i^f - \frac{P_i^h}{\iota_i}} \tag{2.4}$$

where ι_i is an efficiency of the conventional heating generating systems.

The power to heat ratio ζ_i is the ratio of the net heat and power outputs. It is an important parameter coupling the heat and power generation, and is assumed as a constant for each CHP unit. The calculation is as follows:

$$\zeta_i = \frac{P_i^e}{P_i^h} \tag{2.5}$$

2.3 Wind Turbine

Wind turbines are widely used in remote areas and can transform the kinetic energy of wind to power. The blades in a wind turbine is connected to a shaft, and is then connected to a generator. The cost of wind power has been decreasing in recent years. However, a notable shortcut is the intermittent nature of electricity generation from wind, which cannot be controlled or stored except with energy storage systems. The generation is not always simultaneous with the electricity demand.

There are two widely used methods to include wind generation into the modelling and calculation of microgrid asset planning. One way is to use the wind output data directly, as is used in [9] and this thesis. Another way is to convert the wind speed data into the wind generation output, which provides a better understanding to the wind power data and can be used in the prediction of the wind power. A commonly used model is the Weibull distribution function. The Weibull distribution of the wind speed uncertainty is given in [12]:

$$\varphi_v(v) = k/\lambda(\frac{v}{\lambda})^{k-1}\exp[-(\frac{v}{\lambda})^k] \tag{2.6}$$

in which v is the wind speed and k and λ are the coefficients. The parameter k influences the shape of the curve and takes a value between 1 and 3. A smaller k corresponds with more variable wind, and a bigger k represents more stable wind power. The parameter λ is proportional to the mean wind speed. The typical curve of the distribution function is shown in Figure 2.2, in which λ is equal to 6.21, and k is equal to 2, which entails a mean wind speed of 5.5 m/s [13].

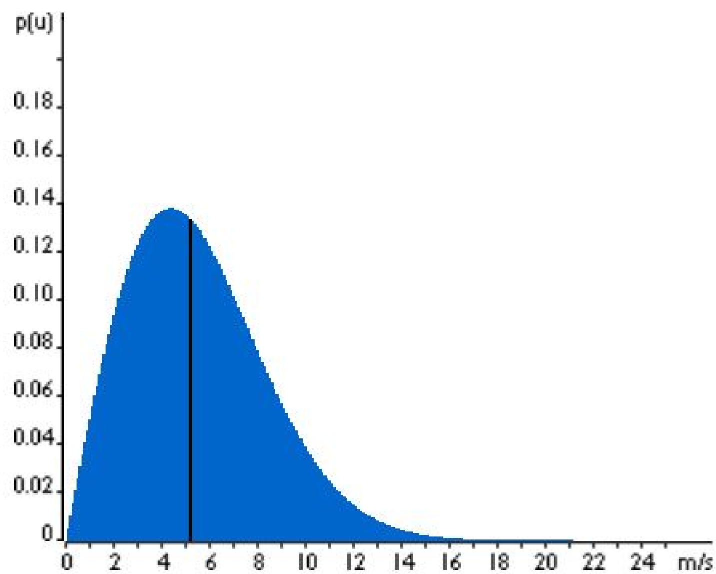

Figure 2.2: Weibull Distribution Function.

The Weibull distribution function is the probability density function (PDF). The idealized power curve is shown as in Figure 2.3 [14]. Before the cut-in wind speed, no electric power is generated. When the rated speed is reached, the wind turbine operates at the rated power, shedding the excess power. After the cut-out speed, the wind turbine is no longer safe and the generator is shut down and the output is zero again.

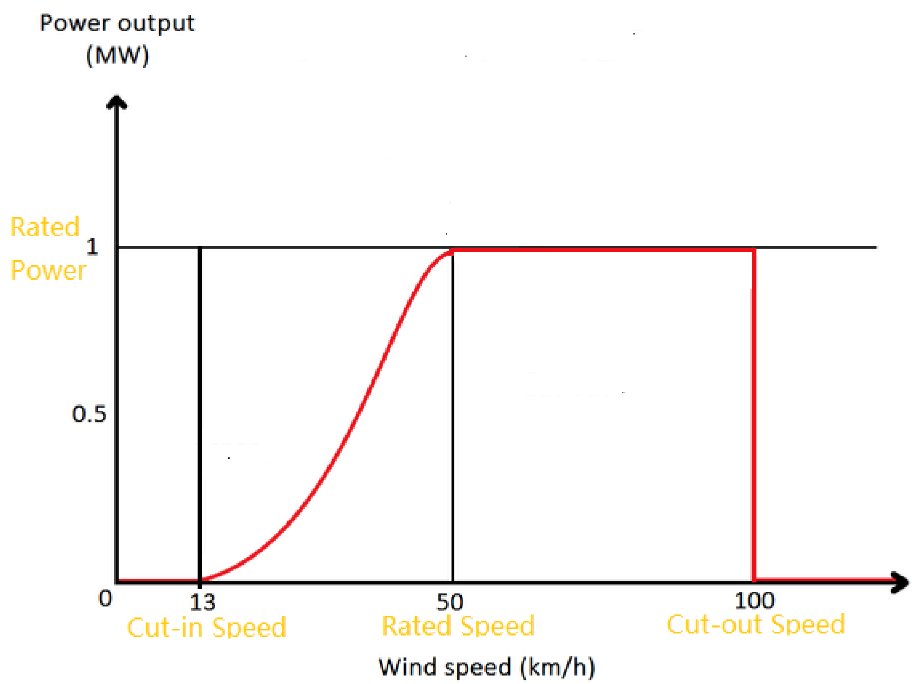

Figure 2.3: Wind Power Curve.

There are other models regarding the wind generation. The probabilistic analytical model in [12] has high efficiency and low computational expense compared with the Monte Carlo method. Similarly, four parameter models for the wind power probability density function are proposed in [15]. In recent years, wind power forecast methods based on machine learning algorithms have shown great benefits over the traditional probabilistic way. Reference [16] proposed a deep-learning-based approach to do the forecast.

The modeling of the relationship between the wind speed and power generation is important for understanding the community microgrid system, while detailed transformation is not in the scope of the thesis. In this thesis, time series data of wind power generation with a time step of five minutes are directly used instead of being obtained from the relationship between wind power and electric power.

2.4 Photovoltaic (PV) Systems

As is similar to the wind generation, there are typically two ways to use the PV generation data in the microgrid. The power output data from the PV plants are directly used in this thesis, but the understanding of the transformation from the environment parameters to the power output is also important, especially in the prediction of PV outputs in the economic dispatch.

PV systems transform energy from sunlight into electricity with PV cells grouped in panels or arrays. The cost of PV products has been greatly reduced with the material replaced from the silicon wafers as is in the microelectronics into high performing thin films [9]. The silicon films are connected to the electric terminals. When the circuit is closed, the PV systems exposed in the sun irradiation generates an electric current from the p-n junction at one of the sides of the silicon layer. Other materials such as gallium arsenide, amorphous silicon and copper indium di-selenide in the multi-junction devices may largely improve the efficiency of the PV system. For the time being, the capital cost of using PV to generate power is relatively higher than many other generating methods including traditional fossil fuel power generation due to the high cost of silicon in the PV arrays.

This thesis focuses on the sizing and economic dispatch in the community microgrid. Similar to the wind power generation, the PV output time series data from the PV power stations are directly used in this thesis, of which the time step is five minutes.

2.5 Energy Storage Systems (ESS)

Energy storage systems are most useful when there is a mismatch between the power production and consumption in the grid. When there exists extra energy in the grid, the ESS stores energy; when the power generation could not meet the demand, the stored energy in ESS can be released. ESS technologies are often used with renewable energy generation so that the maximum potential of the renewable energies can be utilized. In

[9], three types of ESS technologies are introduced. The first type can both withdraw the energy from the grid and re-inject it back, including batteries, flywheels and compressed air. The second type can only withdraw energy from the grid when needed, and then compensate for the energy demand of the host facility directly, rather than re-inject the power into the grid. This kind of ESS includes heat storage and ice production in buildings. The third type of ESS can withdraw energy from the grid and then store the energy as other forms like fuel, steam and other storable types. This thesis focuses on battery-like ESS technologies for the microgrid.

To determine the operating state of the ESS in period t, the energy state at time $(t-1)$ and the charging/discharging power in period t should be known. In [11], the steady state description of the ESS in the sizing problem is provided as the following:

$$
\begin{aligned}
E_i^e(y,t) &= E_i^e(y,t-1) + \eta_i^c P_i^c(y,t)\Delta t - P_i^d(y,t)\Delta t, \\
P_i^e(y,t) &= P_i^c(y,t) - \eta_i^d P_i^d(y,t), \\
0 \leq E_i^e&(y,t) \leq x_i, \\
-v_i x_i \leq P_i^c&(y,t) \leq v_i x_i
\end{aligned}
\tag{2.7}
$$

in which E_i^e is the state of charge at time t, η_i^c and η_i^d are the charging and discharging efficiencies, respectively, and x_i is the storage capacity (in Wh) of the system. The powers P_i^e, P_i^c and P_i^d are the battery net power, charging power and discharging power, respectively. The first and second lines of (2.7) illustrate the relationship between the electrical energy level and the electrical power of the ESS, and the other constraints show the upper and lower limits of the ESS energy and power. The constant v_i (in h^{-1}) indicates the charging/discharging speed and is dependent on the ESS technology. The larger v_i is, the faster the charging or discharging could be.

2.6 Electric Vehicle Charging Stations in Community Microgrids

An electric vehicle charging station (EVCS) is a significant component in community microgrids as they can contribute in exacerbating peak demand problems. To verify whether the microgrid can meet the electric demand of the EVCSs and to investigate the impacts of introducing them, the characteristics of EVCSs are introduced in this section.

2.6.1 Literature Review

Some of the previous studies in the planning model on integrating EV charging stations into the distribution networks are introduced in [17]. Many studies investigate the site selection of charging stations and the planning for fast charging station (FCS) networks. Sizing in [18] includes the traffic flow and charging requirements in the constraints, but does not cover the diversity of travel distances and plug-in electric vehicle (PEV) electric ranges. Siting and sizing of PEV charging stations is discussed in [19–22] to meet the PEV demand. However, the charging station capacity is not considered. In [21], just a fixed number of charging stations are sited in the maximal covering model. Similarly, the PEV demand is not met in the planning model in [18]. In [19], a two-step method taking into consideration of the environmental factors and the service radius of PEV charging stations is considered. In [20], a hierarchical clustering method is adopted for the classification of the Battery Electric Vehicle (BEV) charging demand and then used in the BEV charging station allocation.

Some research works consider the user's behaviors, trip distances and the capacity of charging stations to meet the maximum demand [19, 23–28]. In [29], the electric vehicle charging stations are divided into slow charging facility (SCF), normal charging facility (NCF) and fast charging facility (FCF). The charging demands are divided into residential area, shopping area and office building area, of which the charging demand distribution is obtained by Monte Carlo simulation. The charging and discharging state of electric vehicles is relevant to the electricity consumption in the distribution network [29]. The electric vehicles can discharge into the distribution network when the electric demand is large in the daytime and charge at night when the electricity load is not heavy.

The objectives of the EVCS planning can be different. In [22], the fast charging is regarded as a demand and the number of FCSs are limited by the investment budget. In [24], the costs that could be included in the objective function associated with electric vehicle charging stations are introduced, including the investment, operation and maintenance costs and network losses. The optimization objective in [29] is different from that of this thesis. In [29], the optimization is done from the stand point of the EVCSs, aiming at minimizing the annualized investment and operation cost of the EVCS, the grid reinforcement cost which the EVCSs need to pay and the network loss cost. While in this thesis, the optimal sizing is done for the microgrid assets, the costs related to the charging station are considered only when they are to be paid by the microgrid owner and is integrated into the total costs used before in the sizing.

2.6.2 Modeling of EV Parking Behaviors and Charging Demands

The research on EV parking behaviors and charging demands can be the basis of the EVCS charging/discharging simulations. For the efficiency of the proposed methods, three simplifications are made in [29]. First, the planning horizon of a year is reduced to eight days, which represents the weekdays and weekends of the four seasons. Then the eight representative days are sampled at 15-minute intervals, so each day is divided into 96 time segments. At last, the EV charging demands and loads are regarded as deterministic within each time segment.

To analyze the EV parking behaviors, the distribution of the EV arrival time and parking durations are investigated. The data to obtain these statistical characteristics are from the historical data of fuel-powered vehicles because they have the similar pattern of driving and parking as the EVs and the data are much easier to obtain. Based on the historical data, the distributions are obtained according to three types of land usage.

To model the spatial and temporal distribution of EV charging demands, a Monte Carlo simulation method is used, which is based on two assumptions. First, two characteristics of EV charging behaviors in community networks should be noted: most of the EVs are charged at the travel destinations and the owners prefer the EV to be fully charged at each time. Second, as for the selection of the charging facilities, two principles are proposed according to the SOC of the batteries and the parking durations of the EVs: the selection of the ratings of charging facilities should guarantee that the EV can be fully charged within the parking duration, and then the lowest rating would be selected based on this. It should be noticed that FCFs are not always preferred because of the negative impacts on the economic life of batteries. Also, unnecessary short charging time may lead to extra efforts in time and distance to remove the fully charged EVs before departure, especially for the public charging stations.

The objective is to minimize the existing costs together with the costs related to the EV charging system: the annualized investment and operation cost of EVCSs. The calculations are given in [29], which is the function of the installation number of charging stations in each node. Constraints are also given in [29] which include the power flow balance, voltage magnitude limits, branch current limits, population balance and distance limits of EVs and charging facility requirements. According to the scenarios in which low-power EV charging demands transfer with high-power demands, quantification of charging power in EVCSs is given in [29], but is then proven to have no influence when added to the optimization model.

With these considerations above, the installation numbers of the EVCSs of different ratings can be decided. In the sizing problem, the EVCSs are considered as electrical loads from the perspective of the microgrid.

2.6.3 Consideration on the EVCSs in a Community Microgrid

The electric vehicle charging stations should be considered specially since the charging power can be significantly greater than other loads. Many EVs can charge between 3.3

to 7.2 kW, and the Tesla models can draw more than double the amount of power from a level 2 charger [30] , whereas a 1.5 ton central air conditioner only draws 5.3 kW on average. As both the popularity of EVs and battery capacities grow, the load curves show high daily peaks and significant fluctuation. Therefore, charging loads of the EVCSs should be investigated when integrating them into a community microgrid planning exercise.

The EVCS annual charging data with a time step of one hour is hard to obtain, but many efforts have been made to investigate the probability distribution of the EV behaviors. Reference [31] used the GPS data on 112 private EVs in Beijing, and reference [32] proposed the probability model based on the spatial and temporal distribution traffic data from 2000 cars.

Most of such models are based on the Monte Carlo method. Monte Carlo simulation can generate outputs for random inputs with a certain model. The output can be analyzed further, for example the minimum, maximum, average value and probability distribution of the output values can be assessed. Many research works use the Poisson distribution as the computerized model in the simulation for EVs, but human behaviors may follow non-Poisson statistics and can be better approximated by a heavy tailed or Pareto distribution [33] . In [31] , the Birnbaum-Saunders distribution is used to simulate the daily traveling frequency and the driving mileage, and the traveling duration is modeled with distribution. A location-scale distribution and the normal distribution is also used to model the departure time of each traveling in the morning and afternoon, respectively.

In this thesis, the annual charging demand is considered in the electrical load, and the data is from [32] , which is generated by the Monte Carlo method considering the spatial and temporal distribution of electric vehicles.

2.7 Demand Response in a Community Microgrid

To address the mismatch between supply and demand, microgrids can not only use distributed energy resources, but also make use of demand side response. Demand response is the most popular demand side management technique. It is the activity that the electricity market customers respond to the time-based price changes or the incentive-based programs. The loads with low priority would participate in the demand response, so that the intelligent systems are allowed to cut them off when the electricity price is high.

The energy available for demand response is also limited. The formulations follow those in [11]. Equations (2.8)-(2.10) show the constraints for the electrical demand response resources. The electrical DR energy already interrupted at time t in (2.8) is dependent on the electrical output P_r^e from DR. Constraint (2.9) outlines the maximum limit of the interrupted DR energy, and the electrical power available for DR are limited by (2.10). The parameter k_r^e is the electrical DR energy to power ratio and is subject to change on different DR technologies. In this thesis, the value of k_r^e is 0.5. The parameter ω_r^e is the percentage of electrical load available for DR and the value is 0.2 in this thesis. Finally, $L^{e,max}$ is the peak electrical load. It is assumed that there is no efficiancy loss in the electrical DR process for simplicity.

$$E_r^e(y,t) = E_r^e(y,t-1) + P_r^e(y,t)\Delta t \tag{2.8}$$

$$0 \leq E_r^e(y,t) \leq \omega_r^e L^{e,max} \tag{2.9}$$

$$-k_r^e \omega_r^e L^{e,max} \leq P_r^e(y,t) \leq k_r^e \omega_r^e L^{e,max} \tag{2.10}$$

Similarly, the thermal load DR constraints are outlined in (2.11)-(2.13). Same as in the electrical DR process, there is no efficiancy loss in the thermal DR.

$$E_r^h(y,t) = E_r^h(y,t-1) + P_r^h(y,t)\Delta t \tag{2.11}$$

$$0 \leq E_r^h(y,t) \leq \omega_r^h L^{h,max} \tag{2.12}$$

$$-k_r^h \omega_r^h L^{h,max} \leq P_r^h(y,t) \leq k_r^h \omega_r^h L^{h,max} \tag{2.13}$$

2.8 Chapter Summary

In this chapter, components of community microgrids are introduced. The mathematical models and characteristics of the dispatchable and non-dispatchable generation resources are outlined. Constraints for demand response are also introduced. As a significant component in community microgrids, modeling of EVCSs and the optimization objectives are explained. The main grid is modeled as a flat power profile, which can be zero or non-zero. This chapter provides a basic understanding of the community microgrid by modeling the energy resources, and the load and generation characteristics are further discussed in Chapter 3.

Chapter 3

Asset Sizing Data Requirements and Analysis

The inputs for optimal sizing are from three types of data: the annual time series data, the typical day time series data and the typical scenario data. The original data of a whole year is the realistic data, which can show the fluctuation characteristics of load and generation, as well as represent possible actual operation of the microgrid. To reduce calculation time and boost algorithm efficiency, the typical day method and the typical scenario method can also be used. The typical day method takes the average data in a month or a season as typical days, while the scenario method generates typical scenarios of load and generation synchronously based on historical data.

In [34], the average of the load profiles of weeks within each season is regarded as representative. Consequently, the operating costs are weighted by the number of weeks for each season in the objective function. Also, an extreme week is added to represent the weeks with extreme variations in load and renewable intermittent generations. However, this method is not accurate enough in dividing the months to take the average values. For example, it is usually assumed that the winter is from December to February, but this is not a rigorous division. The same problem also applies to other seasons if a closer look at the yearly climate data is taken.

A better way to scale down the size of data is proposed in [35], in which the classification is not pre-defined, but generated with a clustering algorithm. To illustrate the method of clustering in the preprocessing of data for asset sizing, a case study which includes PV, wind and CHP units is taken as an example. The electricity load, the wind generation and the PV generation are considered together to guarantee their time labels are the same after scaling down the data size. Their time steps are all for an hour and the data is available for a whole year.

In this chapter, analysis of the input data is investigated so as to determine whether the reduced data or the original data should be used in asset sizing. The k-means clustering method [36] is used in analysis.

3.1 Electrical Load Data

In this section, the pattern of a typical electrical load is studied to illustrate the characteristics of the community electricity consumption. The data is from the urban area of Calgary, Alberta [9]. The load data are clustered with a dimension of 365 days of 24 hours (i.e., 8760 hours). According to the silhouette scores (a measure of how close a data point is to its own cluster) when the number of clusters are chosen within a range from 2 to 9, the best two clustering results are obtained when the load profiles are divided into three or two groups, as is shown in Table 3.1.

Table 3.1: Silhouette Scores

Number of Clusters	2	3	4	5	6	7	8	9
Silhouette Score	0.5372	0.5166	0.4456	0.4570	0.4550	0.5035	0.4951	0.4893

Calculation for the silhouette score $s(i)$ is shown in (3.1) for data point $i \in C_i$ (data point i in the cluster C_i).

$$
\begin{aligned}
a(i) &= \frac{1}{|C_i| - 1} \sum_{j \in C_i, i \neq j} d(i,j), \\
b(i) &= \min_{k \neq i} \frac{1}{|C_k|} \sum_{j \in C_k} d(i,j), \\
s(i) &= \frac{b(i) - a(i)}{\max\{a(i), b(i)\}}, \text{ if } |C_i| > 1, \\
s(i) &= 0, \text{ if } |C_i| = 1
\end{aligned}
\tag{3.1}
$$

in which $d(i,j)$ is the distance between data points i and j, and C_k represents all the clusters other than C_i ($C_k \neq C_i$).

The result in Table 3.1 is validated with the elbow method [37]. To find the optimal number of clusters, k, a line chart of the sum of square errors is plotted for each k in a range of values. The line chart typically looks like an arm, and the ”elbow” on the arm correspond to the optimal value of k. In this case, the best number of clusters, i.e. the optimal k value, is found to be two or three, as is shown in Figure 3.1.

The electrical load profiles are clustered into three groups, as is shown in Figure 3.2. The dotted lines indicate the average of the respective clusters. The blue one represents a pattern with a high and steady consumption during the daytime. This may correspond to winter when heating is greatly needed. The green one shows the usage which is also relatively high, but with two peaks in the early morning and late afternoon, which is related to spring and fall when people turn off their heating devices, leave home for work or study and come back at night. The purple one is relatively low throughout the day and corresponds to summer. For all the three clusters, even in the valley of usage, there remains some level of consumption, since there exists some usage of commercial electricity in the community, rather than merely residential loads.

The results of clustering are also shown in Figure 3.3 when the number of clusters is equal to two. In this case, the silhouette score is slightly higher than that when the loads are clustered into three groups, but the results can be less obviously interpreted.

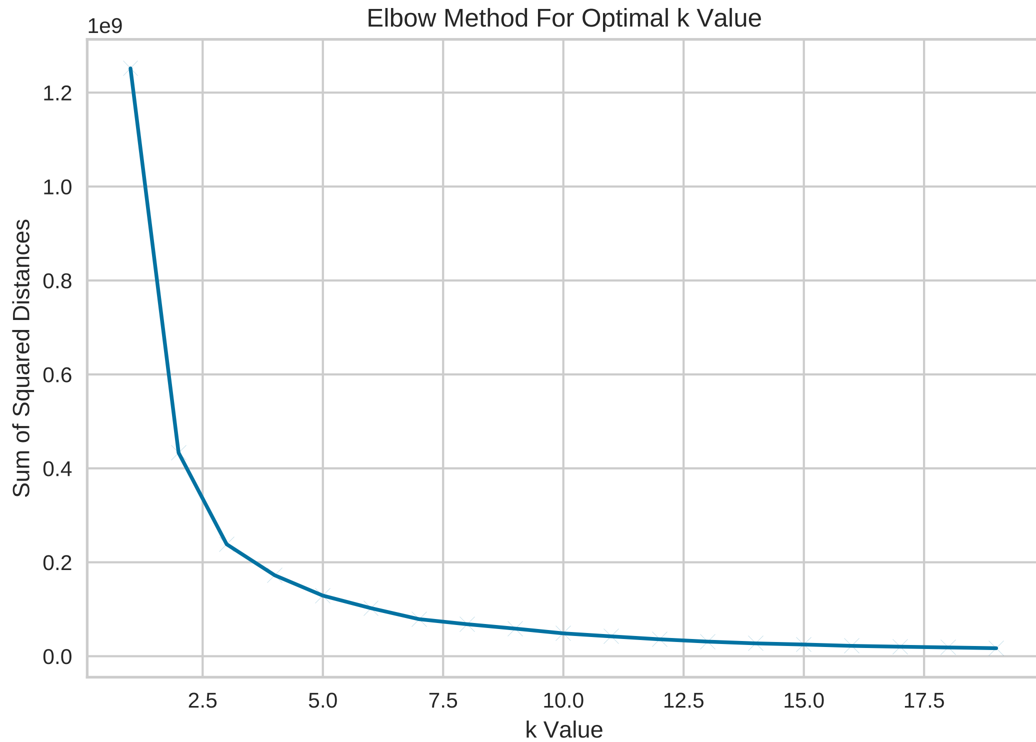

Figure 3.1: Optimal k Value for Electrical Load.

3.2 Net Load Data

The input data in the asset sizing problem include the electrical load as well as PV and wind generation. The net load in the typical community microgrid is the electrical load minus PV and wind generation. To explore the possibility of simplifying the input data, the clustering method is used on the net load data.

3.2.1 Demand-Wind-PV Data

The first attempt to cluster the whole input data is done with the Demand-Wind-PV data all involved. For 1 p.u. of the maximum demand, the maximum of wind generation is 0.45 p.u. and that of PV is 0.19 p.u. The scaled data of the electrical load, wind generation and PV generation are plotted in Figure 3.4. It is easy to observe that the data of the wind

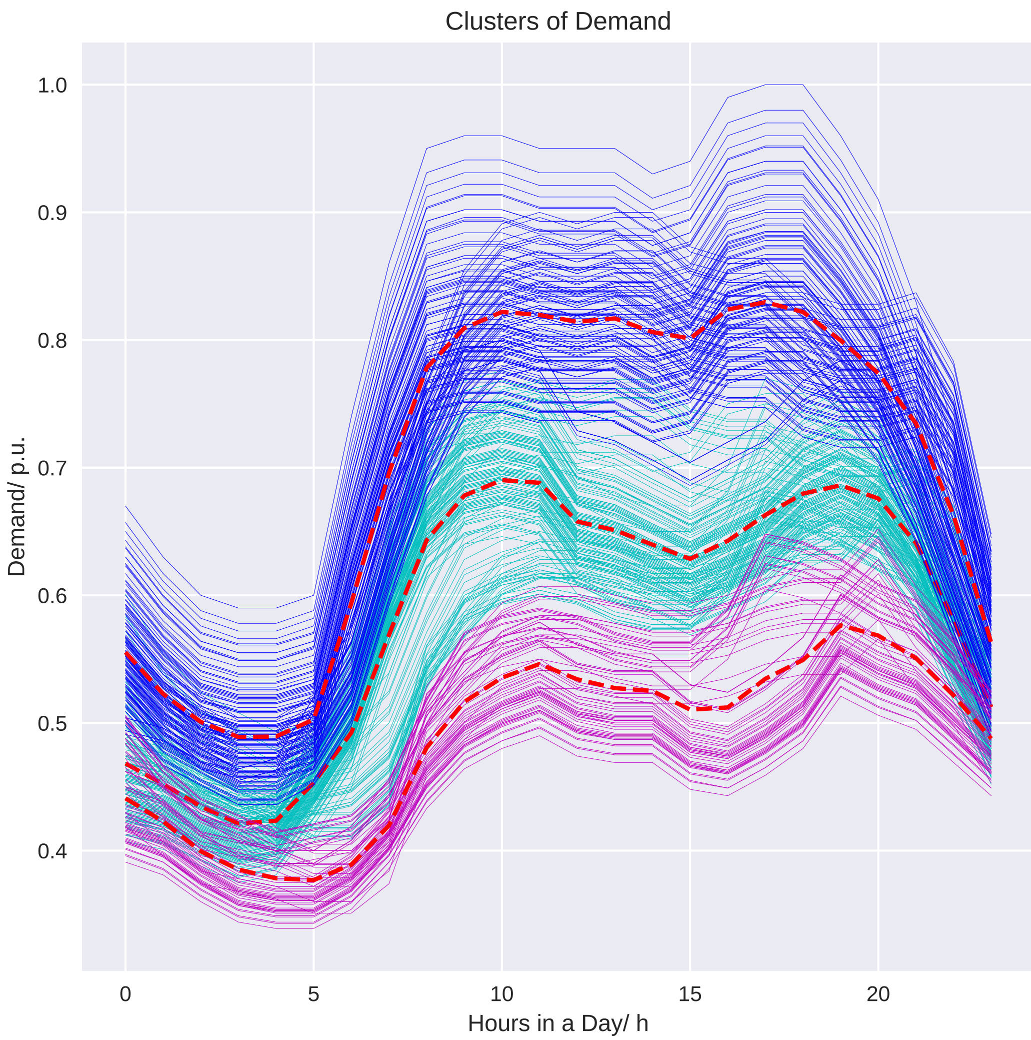

Figure 3.2: Clusters of Demand (k=3).

generation may not follow some obvious patterns as the electrical load and PV generation do. This is also shown in Figure 3.5. It may still make sense to perform clustering, for the machine learning algorithms may dig out some characteristics of the data, yet it is hard to draw any conclusion just by observation.

For better observation, a three-dimensional plot of the data is shown in Figure 3.6. As is the same with two-dimensional plots, the electrical load may be clustered into three

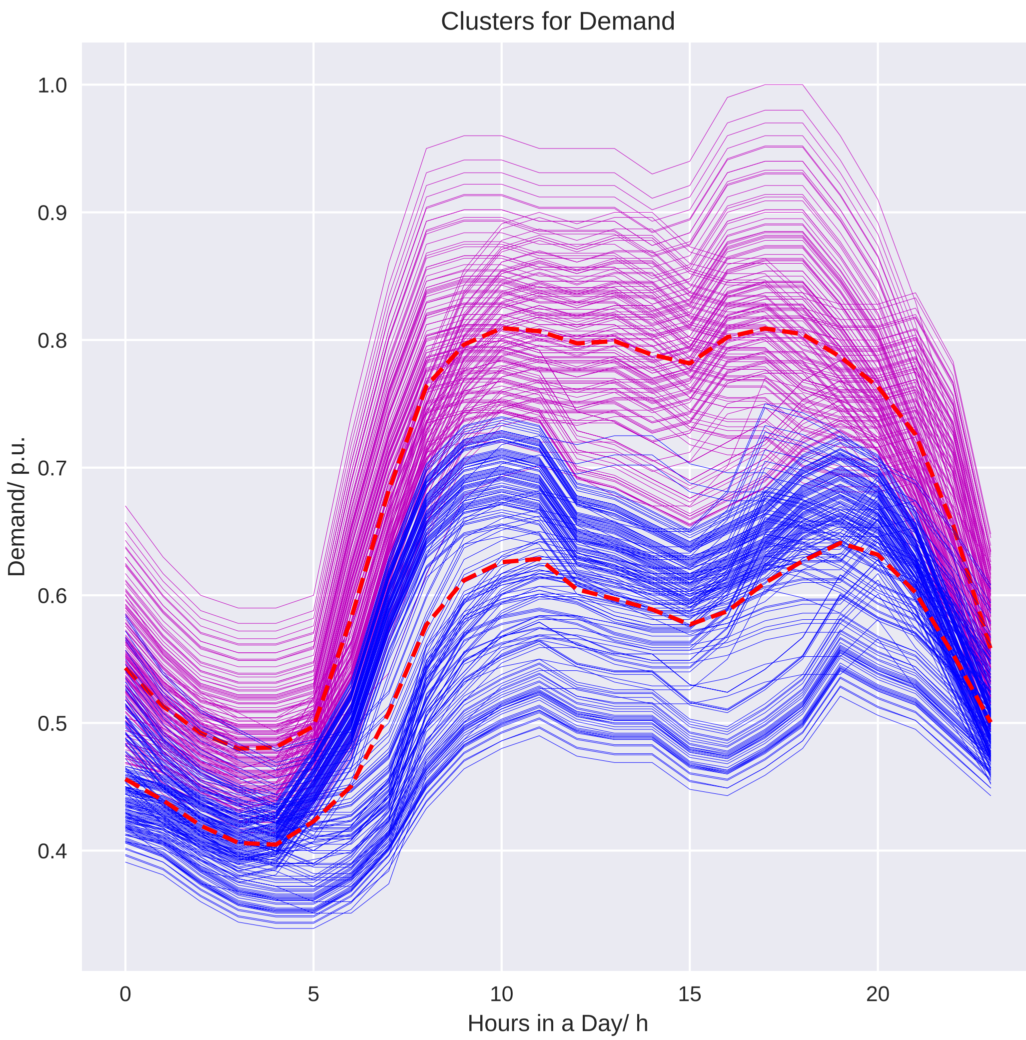

Figure 3.3: Clusters of Demand (k=2).

groups, and PV generation may also follow some patterns. However, wind generation is in a chaos. Therefore, to determine the number of clusters, the silhouette score method and the elbow method are used.

The silhouette scores corresponding to different numbers of clusters in a range from 2 to 33 is listed in Table 3.2. As can be seen, the highest silhouette score is taken when there are only two clusters. This value is just slightly higher than 0.5, which is the boundary

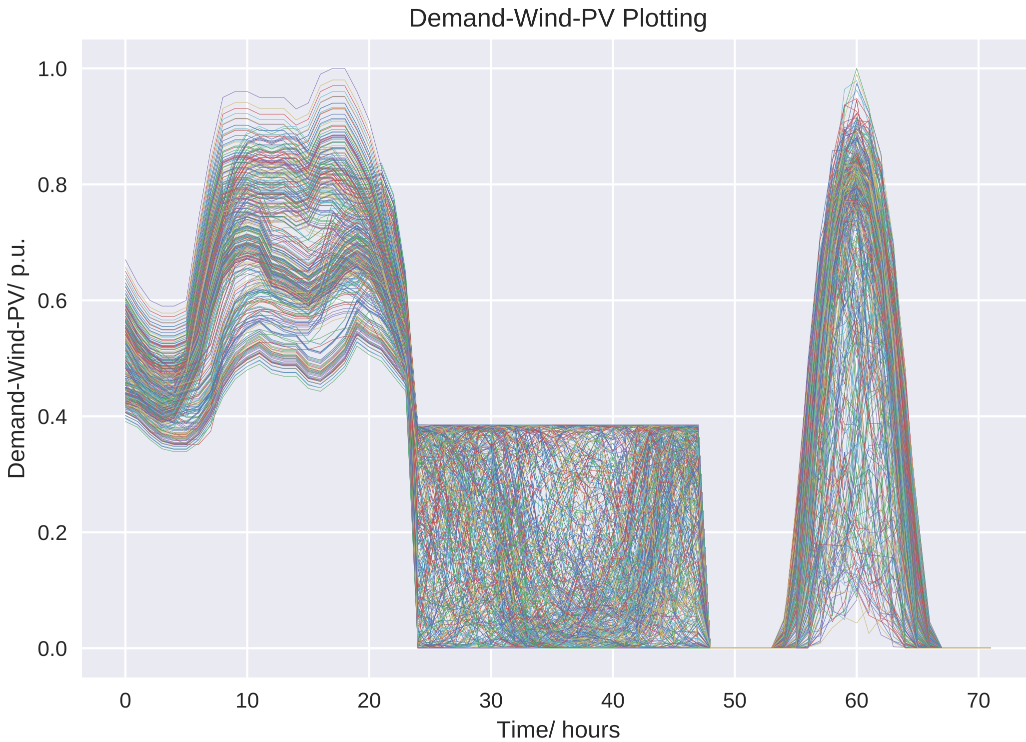

Figure 3.4: Data Plotting of Demand-Wind-PV.

Table 3.2: Silhouette Scores

Number of Clusters	2	3	4	5	6	7	8	9
Silhouette Score	0.5368	0.5149	0.4448	0.4554	0.4527	0.4989	0.4900	0.4760
Number of Clusters	10	11	12	13	14	15	16	17
Silhouette Score	0.4943	0.4981	0.5054	0.5157	0.5144	0.5174	0.5066	0.5056
Number of Clusters	18	19	20	21	22	23	24	25
Silhouette Score	0.4973	0.4934	0.4849	0.4863	0.4923	0.4837	0.4755	0.4854
Number of Clusters	26	27	28	29	30	31	32	33
Silhouette Score	0.4846	0.4818	0.4912	0.4908	0.4906	0.4810	0.4884	0.4975

value deciding whether the partition of data is reasonable. Also, it is obvious that the data of 365 days could not be represented by data representing only two days in the sizing problem. Therefore, the clustering method for the Demand-Wind-PV data is not suitable for this case study of community microgrid.

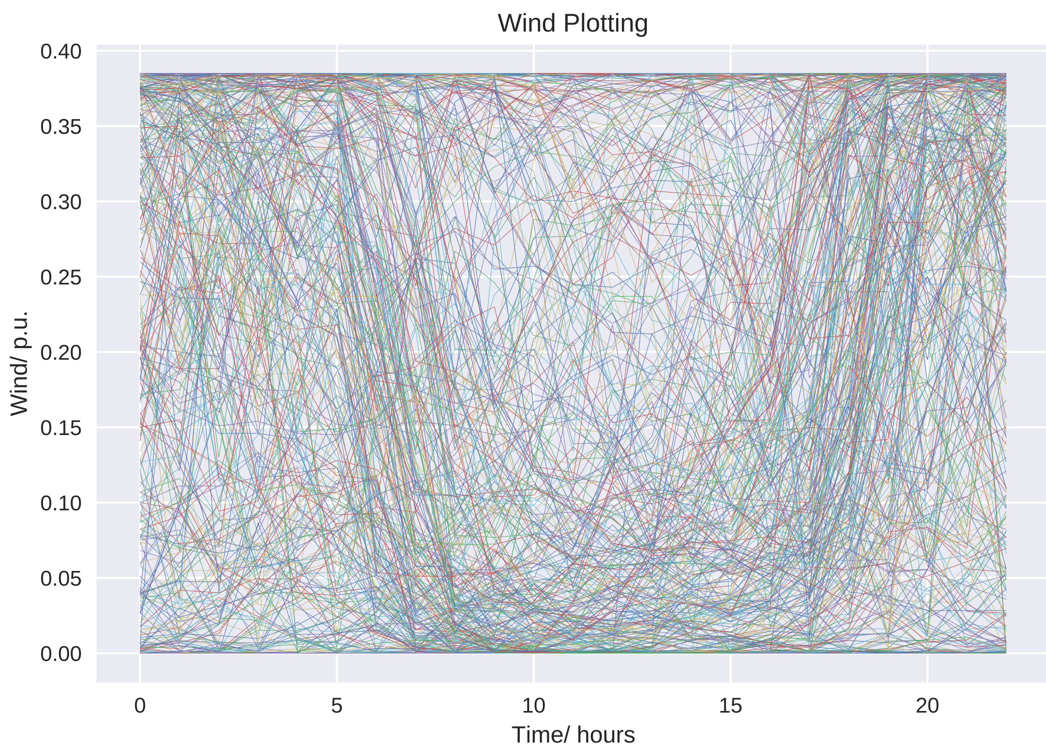

Figure 3.5: Data Plotting of Wind Generation.

The result can be validated by the elbow method. As can be seen in Figure 3.7, the elbow point is taken when the number of clusters is two.

Even if k-means clustering is substituted by agglomerative clustering, the silhouette scores when the number of clustering is taken from 2 to 33 show a similar result that the optimal number of clustering is 2, as is in Table 3.3. Obviously, this does not make sense in the asset sizing problem because the clusters are too rough.

3.2.2 Demand-PV Data

In [35], a wind-irradiation-load typical scenario clustering method is proposed with a two-step clustering method. The Demand-Wind data are clustered first and the cluster centers are then combined with the wind speed data to do further clustering. The reduced planning data could approximate the original scenarios to find the optimal configuration

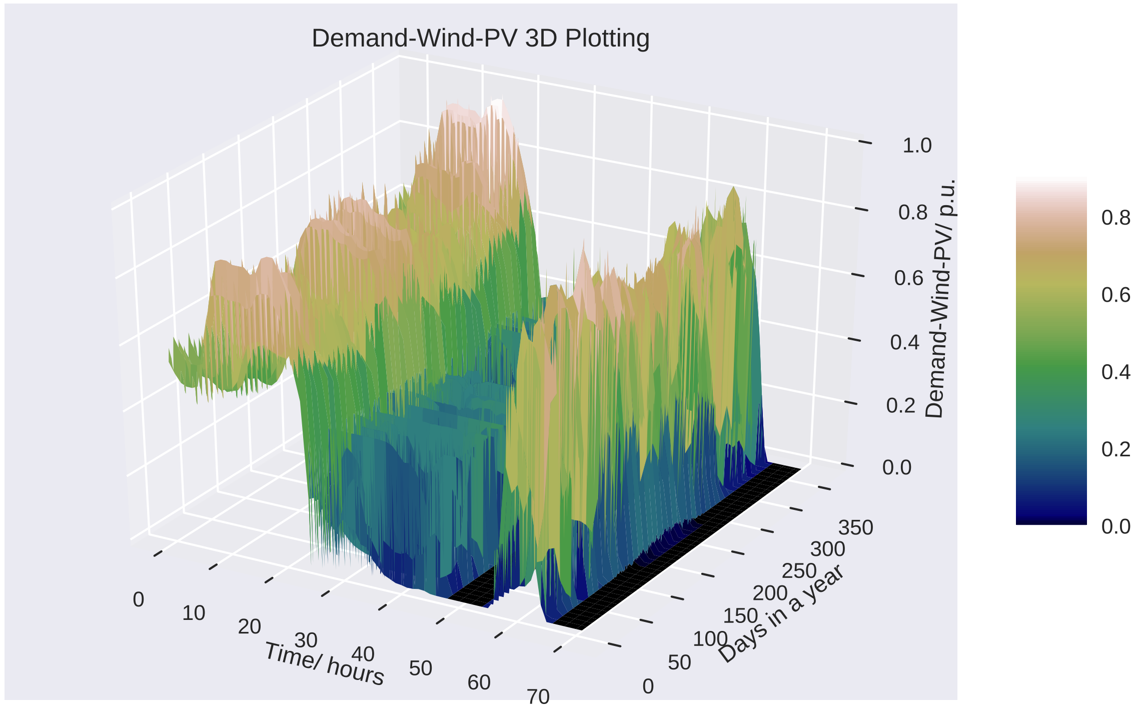

Figure 3.6: 3D Data Plotting of Demand-Wind-PV.

Table 3.3: Silhouette Scores

Number of Clusters	2	3	4	5	6	7	8	9
Silhouette Score	0.5356	0.4827	0.4309	0.4417	0.4737	0.4637	0.4632	0.4611
Number of Clusters	10	11	12	13	14	15	16	17
Silhouette Score	0.4632	0.4584	0.4749	0.4875	0.4942	0.4921	0.4892	0.5062
Number of Clusters	18	19	20	21	22	23	24	25
Silhouette Score	0.4874	0.4714	0.4817	0.4806	0.4802	0.4814	0.4845	0.4769
Number of Clusters	26	27	28	29	30	31	32	33
Silhouette Score	0.4830	0.4857	0.4792	0.4777	0.4797	0.4862	0.4856	0.4854

of the renewable energy resources. In this section, the Demand-PV data is clustered as is done in [35], as the first attempt of the two-step clustering method.

The silhouette scores are studied to find the best number of clustering, and a set of data is taken as an example in this section. As is shown in Table 3.4, even though the

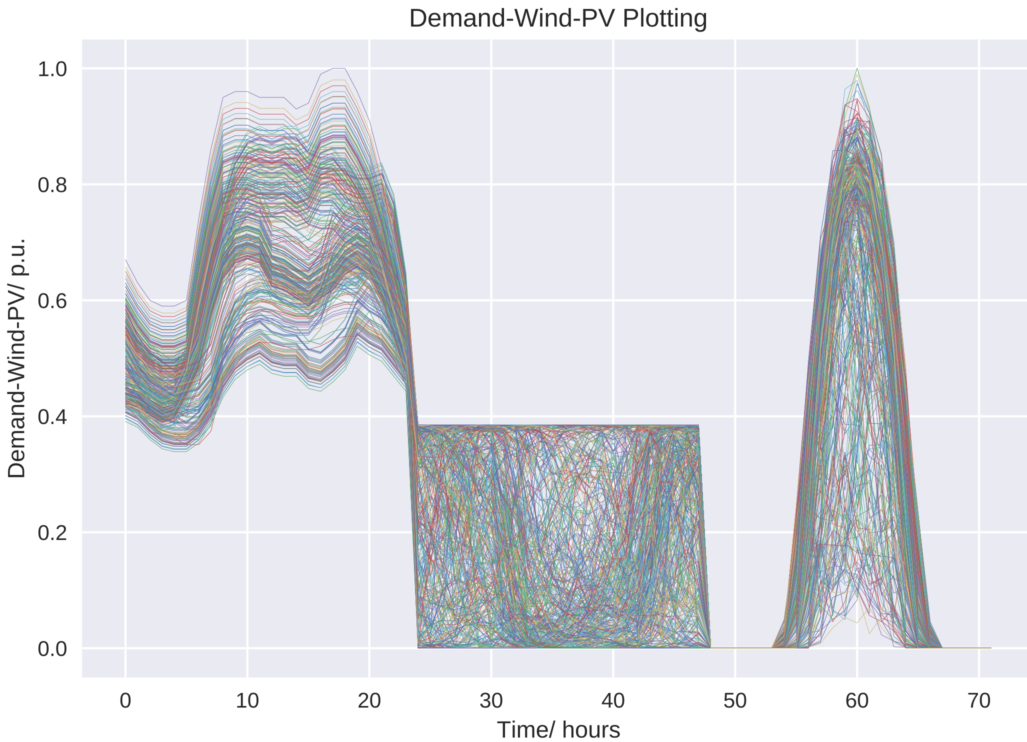

Figure 3.7: Elbow Method for the Demand-Wind-PV Data.

Table 3.4: Silhouette Scores

Number of Clusters	2	3	4	5	6	7	8	9
Silhouette Score	0.5372	0.5156	0.4456	0.4571	0.4531	0.5023	0.5023	0.4732
Number of Clusters	10	11	12	13	14	15	16	17
Silhouette Score	0.5002	0.5054	0.5089	0.5159	0.5185	0.5302	0.5316	0.5137
Number of Clusters	18	19	20	21	22	23	24	25
Silhouette Score	0.5116	0.5029	0.4889	0.4825	0.5025	0.5045	0.4993	0.5008
Number of Clusters	26	27	28	29	30	31	32	33
Silhouette Score	0.4962	0.4972	0.5022	0.4920	0.5048	0.5078	0.5050	0.5074
Number of Clusters	34	35	36	37	38	39	40	41
Silhouette Score	0.5232	0.5135	0.5338	0.5167	0.5239	0.5368	0.5430	0.5463
Number of Clusters	42	43	44	45	46	47	48	49
Silhouette Score	0.5268	0.5403	0.5374	0.5331	0.5259	0.5434	0.5417	0.5491

chaotic wind data is taken out of the input, the clustering result is still not desirable. For the number of clusters less than 39, the highest value of the silhouette score is also taken at two. Similarly, the result of the elbow method is shown in Figure 3.8, and The elbow point is taken at two. Better results occur only when the number of clustering is larger than 40, which is a good result compared with the original size of 365 data points. This may be because the PV has a seasonality pattern simillar with demand and at least three scenarios are needed. Considering the variability in each cluster, extra scenarios are needed.

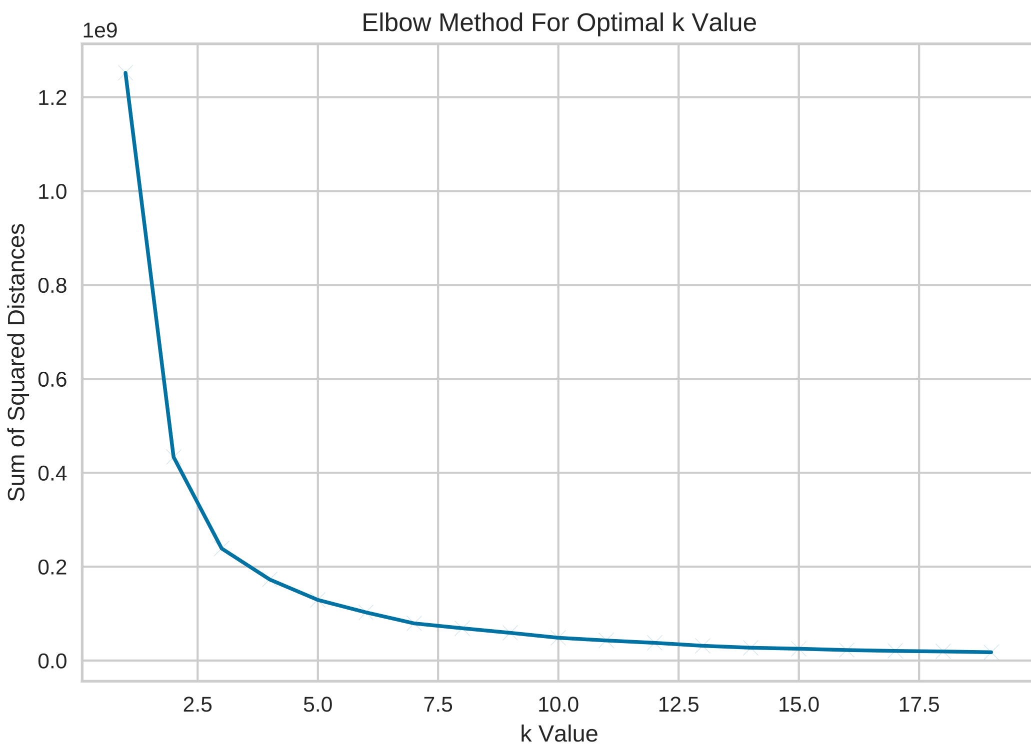

Figure 3.8: Elbow Method for the Demand-PV Data.

However, until the number of clusters is as large as 49, the silhouette score is just slightly higher than 0.5 (no more than 0.55), which is not an ideal score [38]. Therefore, for this data set, the Demand-PV data should better not be clustered to serve as the input data of the two-stage clustering method proposed by [35]. Then, if the calculation time is undesirable, the clustering method would be considered again. For this data set, the asset sizing problem with the original data for five years can be solved within one minute with modern linear programming solvers, as can be seen in Section 4.3, thus the clustering would not be performed. However, if the given data have a longer time span or a clearer clustering pattern, the choice may be different.

3.3 EVCS Data

An example of data of EVCS annual charging demand is from [32]. Demands for 33 nodes in [32] are added up, taking 500 electric vehicles into consideration. The time step is one hour, and there are 8760 time points in a year in total. As is plotted in Figure 3.9, the charging power curve can be very sharp with obvious peaks, especially when fast charging stations are included in the system. The average is below 80 kW but the peak can be higher than 200 kW. This is a significant challenge for community microgrids.

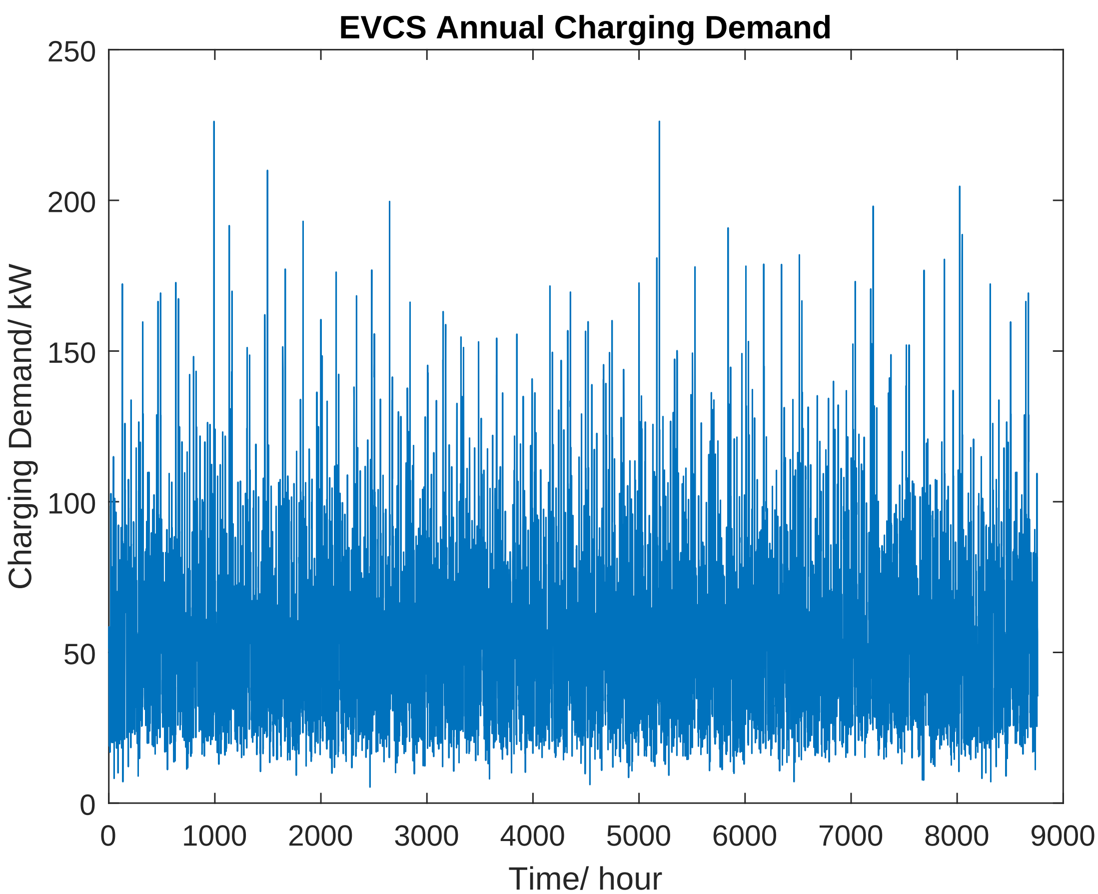

Figure 3.9: EVCS Annual Charging Demand.

Figure 3.10 shows the comparison of the load data within a typical day without and with EVCSs. It is obvious that the EVCSs added irregular components to the electrical load and the peak is 3.1% higher than before. This is discussed further in the community microgrid sizing in the next chapter.

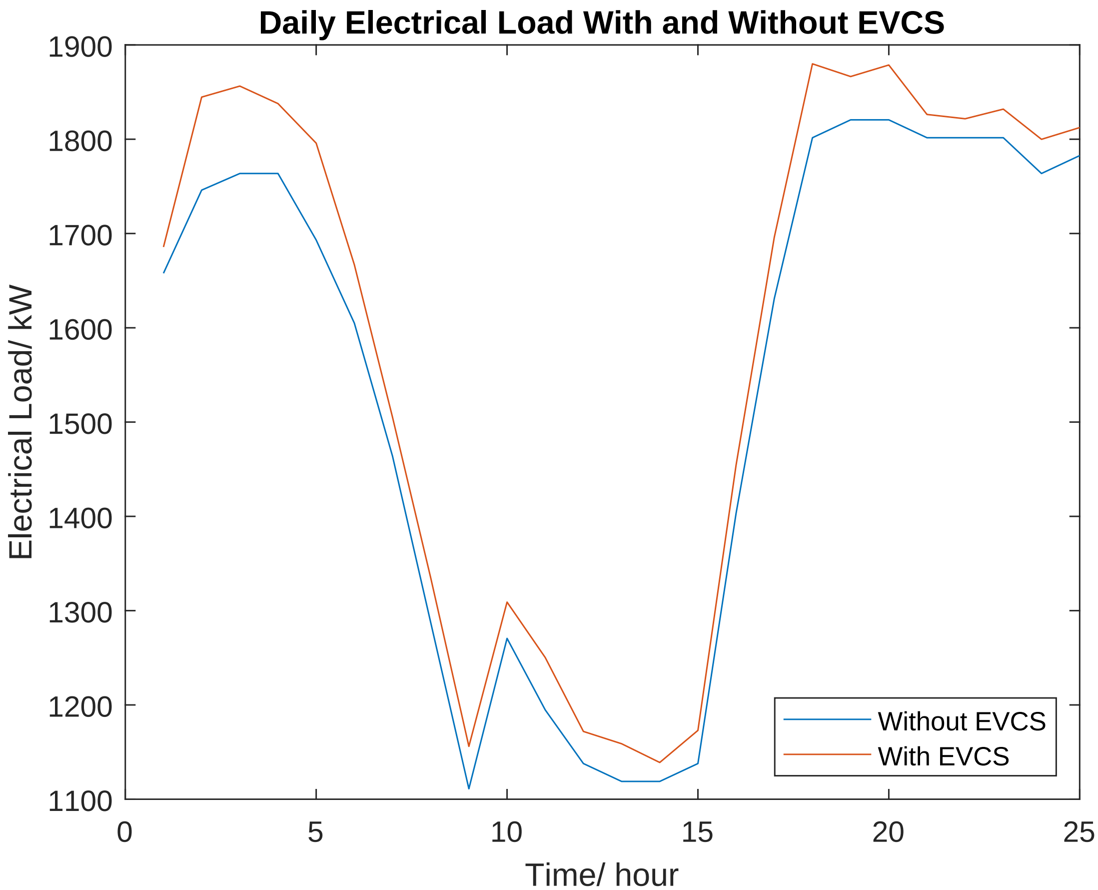

Figure 3.10: Daily Demand With and Without EVCS.

3.4 Chapter Summary

In this chapter, a typical set of input data of the asset sizing problem is analyzed in order to decide whether the original data or the representative data should be used later.The demand data, Demand-Wind-PV data and Demand-PV data are clustered with machine learning methods. Also, the impacts of the EVCSs in the community microgrids are presented. Generally speaking, if data sets are clustered, the calculation time would be shortened greatly, but sometimes algorithms fail to give good clusters for some data. If data sets presenting each day are chosen as inputs rather than clustered data, a large number of possible input profiles are included, but the calculation time would be long for massive data. Choices would be made based on characteristics of specific data sets. Based on the discussion of input data in this chapter, the asset sizing case studies are done in Chapter 4.

Chapter 4

Community Microgrid Asset Sizing

4.1 Introduction

To integrate distributed energy generation and other technologies into community microgrids, studies have to be done to optimize economic and environmental objectives through adequate methods of asset sizing and energy management. Reference [9] proposes a bi–level formulation for microgrid power and reserve capacity planning problems and validates it on a Canadian utility microgrid. The distribution system operator is considered in the lower level problem, while in [39], the microgrid asset sizing problem and the distribution system operators are considered together in a multi-objective optimization method. In [40], a mixed-integer linear programming approach is used in an optimal energy storage sizing method, and case studies are done on an islanded microgrid with PV generation and batteries, but the demand of only ten residential customers is included. In [41], a sizing and control method of an islanded microgrid including wind generation and ESS is done, and reliability requirements of the microgrid are considered.

In this thesis, the asset sizing method proposed in [11] is used in community microgrids. In this chapter, the formulations are introduced and the algorithm is tested on several case studies.

4.2 Community Microgrid Asset Sizing Formulation

The asset sizing problem is aimed at minimizing annualized investment and operational costs, including the annual investment cost of new DER resources, cost of electricity purchased from the main grid, sum of hourly electricity and heat generation costs within a year and the maintenance cost of existing and new generation units. The formulations of the investment cost, the operational cost and the total cost, which has to be minimized, are shown in (4.1)-(4.3).

$$C_{in} = \gamma \sum_{Y} \{\rho_Y (\sum_{S} C_S^c x_S) + D_Y R_Y\} \tag{4.1}$$

$$C_{op} = \sum_{t,y} C_{die} P_{ed}(t,y) + \sum_{t,y} C_{gas} P_{eCHP}(t,y) + \sum_{t,y} C_{gas} P_{hnonCHP}(t,y) + \sum_{S} C_m x_S \tag{4.2}$$

$$min \quad C_{total} = C_{in} + C_{op} \tag{4.3}$$

in which the investment cost C_{in} is annualized by factor γ [11], and ρ_Y is the capital recovery factor. The set S represents ESS devices, and C_S^c and x_S represent capital costs and capacities of set of all sources, including diesel generators, ESSs, CHP units, PV and wind generation. Parameters D_Y and R_Y represent demand charge per kW from the main grid and the maximum annual kW demand from the main grid, respectively. Purchasing cost of carbon permit is included in the operational cost in the form of fuel costs. In (4.2), the operational cost C_{op} is influenced by C_{die}, C_{gas} and C_m, i.e. operational costs of diesel generators, gas generators and ESSs, respectively. Variables P_{ed}, P_{eCHP} and $P_{hnonCHP}$ represent power output of diesel generators, power of CHP units and heat output of non-CHP units in each time point t of each year y. The objective is to minimize the total cost C_{total} in (4.3).

Constraints of the asset sizing problem are listed in (4.4)-(4.11). Constraints (4.5)-(4.11) apply for all the time t and year y. Constraint (4.4) is the budget constraint of the total capital costs and C_b is the budget. Constraints (4.5) and (4.6) represent power and thermal balance equations, in which P_{ew}, P_{ePV}, P_{erc} and P_{es} represent power from wind generation, PV generation, the main grid and ESS. Variables L_e and L_h are electricity and thermal loads. Similarly, P_{hCHP} and $P_{hnonCHP}$ are thermal power from CHP units and non-CHP units. Constraint (4.7) shows the relationship of electric and thermal power generated by CHP units, and ζ is the power to heat ratio, as is introduced in Section 2.2.

$$\sum_S C_S^c x_S \leq C_b \tag{4.4}$$

$$P_{eCHP}(t,y) + P_{ed}(t,y) + P_{ew}(t,y) + P_{ePV}(t,y) + P_{erc}(t,y) = L_e(t,y) + P_{es}(t,y) \tag{4.5}$$

$$P_{hCHP}(t,y) + P_{hnonCHP}(t,y) = L_h(t,y) \tag{4.6}$$

$$P_{hCHP}(t,y) = P_{eCHP}(t,y)/\zeta \tag{4.7}$$

All the demands, PV and wind generation are supposed to be represented for every hour of every year in the planning. In Section 4.3, case studies are presented on a five-year hourly dataset.

Maximum power limits for diesel generators, wind and PV generation as well as CHP units are shown in (4.8)-(4.11).

$$P_{ed}(t,y) \leq x(diesel) \tag{4.8}$$

$$P_{ew}(t,y) \leq x(wind) \tag{4.9}$$

$$P_{ePV}(t,y) \leq x(PV); \tag{4.10}$$

$$P_{eCHP}(t,y) \leq x(CHP); \tag{4.11}$$

Constraint (4.12) limits the maximum energy of ESSs, i.e. state-of-charge (SoC), which is decided by SoC of the former time, the charging and discharging efficiency and the charging power. Constraints (4.13)-(4.15) limit the charging power. Details of (4.12)-(4.15) are given in the illustration of (2.7) in Section 2.5.

$$0 \leq E_{es}(t,y) \leq x(ESS) \tag{4.12}$$

$$E_{es}(t,y) = E_{es}(t-1,y) + \eta^c P_{es}^c(t,y)\Delta t - P_{es}^d(t,y)\Delta t \tag{4.13}$$

$$P_{es}(t,y) = P_{es}^c(t,y) - \eta^d P_{es}^d(t,y) \tag{4.14}$$

$$-vx(ESS) \leq P_{es}(t,y) \leq vx(ESS); \tag{4.15}$$

Similarly, the energy and power of DR are limited. The formulation of DR are illustrated in (2.8)-(2.13) in Section 1.3.7.

4.3 Asset Sizing Results and Discussion

In this section, case studies are run on a community microgrid with different components. Data for electric and heat load is from [9]. PV and wind generation data is from [42] and is normalized to the range [0,1]. Charging/discharging data of EVCSs with a maximum value of 226 kW is found in [32]. The value of the discount rate ρ_Y is 0.9661 as is in

[9]. Case I-VI investigate a community microgrid in the island mode. Case I, the baseline case, only considers diesel generators, wind generation and energy storage systems in the microgrid. In Case II, PV generation is added to investigate the influence of adding an intermittent renewable energy source, especially how the costs and capacities of other components would change. In Case III, combined heat and power (CHP) units are added on the basis of Case II. Although CHP is not a renewable energy source, it serves as a way to boost the efficiency of energy utilization, thus reducing the total cost. To validate that ESSs are significant to the community microgrid with renewable energy sources integrated, Case IV takes out the ESS from components in Case III to see how the results would change. In Case V, demand response (DR) is added into Case III. The community microgrid is run on the grid-connected mode in Case V. Besides, the EVCSs are added based on Case V to see whether the community microgrid can meet the demand of EV charging without incurring significant demand charges from the main grid.

The case studies are implemented on a commercial algebraic modelling tool (GAMS [7]) and a commercial mixed-integer linear programming solver (CPLEX [8]). The results are illustrated in the following sections.

4.3.1 Case I (Baseline): Diesel, Wind and ESS

The system configuration data are obtained from [11]. The capital costs and maintenance costs of the components are shown in Table 4.1 [11].

Table 4.1: Capital Costs and Maintenance Costs

	Capital Cost ($/kW)	Maintenance Cost ($/kWh)
D	1100	0.003
ESS	600	10
CHP	1200	0.006
wind	2213	33
PV	3400	16

Results of capacities and costs are shown in Table 4.2 and 4.3, and the units in Table 4.3 are million of dollars.

Table 4.2: Rating of Each Resource in Case I

Energy Type	D(kW)	ESS(kWh)	CHP(kW)	Wind(kW)	PV(kW)
Rating	1867	1143	0	1000	0

Table 4.3: Investment and Operation Costs for Case I

Total Cost/$MM	20.570
Investment Cost/$MM	11.544
Annual Operation Cost/$MM	9.026

It is the same as the results in [43] that the total capacity of the renewable generation, i.e. wind generation, would be used first because it is involved in the least costs according to the cost function. This would be validated again in Case II, where PV generation is added. An ESS of a capacity of 1143 kWh is used to compensate the fluctuation of wind generation. The rest of the electrical load is met by diesel generators.

4.3.2 Case II: Diesel, Wind, ESS and PV

In Case II, PV generation is added based on Case I. The hourly PV generation data of five years is obtained from [44]. The results are shown in Table 4.4 and 4.5.

Table 4.4: Rating of Each Resource in Case II

Energy Type	D(kW)	ESS(kWh)	CHP(kW)	Wind(kW)	PV(kW)
Rating	1611	3212	0	1000	415

Table 4.5: Investment and Operation Costs for Case II

Total Cost/$MM	25.345
Investment Cost/$MM	17.068
Annual Operation Cost/$MM	8.277

When PV generation is added, the system relies less on diesel generation. The total capacity of the renewable energy, i.e. wind and PV generation, is used first, as is the same as the analysis in [43]. The ESS capacity goes up accordingly to compensate the fluctuation added by PV generation.

Compared with Case I, both the total cost and the operational cost decrease after adding PV generation in the community microgrid. The investment cost increases a little in this case, but it is subject to change given different proportions of energy resources and parameters related to the investment of energy sources.

4.3.3 Case III: Diesel, Wind, ESS, PV and CHP

In the third case, CHP units are added. CHP units can meet the electrical and thermal loads simultaneously, transforming the waste heat in the electricity generation into utilizable heat source to meet the thermal load. The results of Case III are shown in Table 4.6 and 4.7.

Table 4.6: Rating of Each Resource in Case III

Energy Type	D(kW)	ESS(kWh)	CHP(kW)	Wind(kW)	PV(kW)
Rating	591	3211	1110	1000	415

Table 4.7: Investment and Operation Costs for Case III

total cost/$MM	19.007
investment cost/$MM	17.559
operation cost/$MM	1.448

Wind and PV generation and the ESS rating remain the same as is in Case II. However, the size of diesel generation decreases by 66%. The decreased part is substituted by CHP units.

When CHP units are added, the total costs during the planning horizon of five years decreases by around 25% compared with Case II. The investment cost increases slightly but the operational cost goes down greatly. This asset sizing is done on a five-year time scale, and the benefits would be more obvious in the long run when the sizing is done for like 20 years.

4.3.4 Case IV: Diesel, Wind, PV and CHP

In Case IV, the ESS is taken out from Case III. The results show that the solution is infeasible, which means that wind and PV generation should operate together with ESSs to provide energy for the community microgrid in island mode. In grid-connected mode, the main grid can offer balancing. If no PV or wind generation is added, diesel generators would help shave the demand peaks.

4.3.5 Case V: Diesel, Wind, ESS, PV, CHP and DR

In Case V, demand response is added based on Case III. The results are shown in Table 4.8 and 4.9.

Table 4.8: Rating of Each Resource in Case V

Energy Type	D(kW)	ESS(kWh)	CHP(kW)	Wind(kW)	PV(kW)	DR(kW)
Rating	894	86	1017	1000	415	220

Table 4.9: Investment and Operation Costs for Case V

Total Cost/$MM	15.193
Investment Cost/$MM	13.711
Annual Operation Cost/$MM	1.483

It can be seen from the results that with the integration of DR of a capacity of 220 kW, the rating of the diesel generation increases slightly compared with Case III, but the ESS greatly decreases by 97%. Generation of CHP units also decreases, and wind and PV generation still remains the maximum value.

The total cost decreases by 12%. Since part of the load can be met by demand response, the investment cost decreases, but the operational cost increases slightly by 2.7%. Reduction of the costs after adding DR is influenced mostly by the constraints of the energy from the main grid and the purchasing costs.

4.3.6 Case VI: Grid-connected; Diesel, Wind, ESS, PV, CHP and DR

The main grid has an incentive to deliver flat power over time. This thesis focuses on community microgrid asset sizing and economic dispatch, and the main grid is simplified as a constant power profile. When the constant is zero, the microgrid operates in island mode as in Cases I-V.

To indicate the impact of having a non-zero flat power exchange profile with the grid, a case study is carried out in this section, and the power from the grid is set to be equal to the lowest amount of demand in an entire year.

Table 4.10: Rating of Each Resource in Case VI

Energy Type	D(kW)	ESS(kWh)	CHP(kW)	Wind(kW)	PV(kW)	DR(kW)
Rating	90	42	195	1000	415	220

It can be concluded from Table 4.10 that the assets in the microgrid are sized smaller. Wind and PV generation consists of the most of the output power in the microgrid.

Table 4.11: Investment and Operation Costs for Case VI

Total Cost/$MM	6.077
Investment Cost/$MM	6.023
Annual Operation Cost/$MM	0.537

The demand charge is 2.2 $/kW and the price of grid energy is 0 $/kWh, which means the costs in Table 4.11 do not cover the expenses of purchasing electricity from the main grid. It is clear that the costs on the microgrid side is largely reduced with the decrease of asset sizing, and the overall cost considering the purchasing cost also depends on the electricity price on the main grid side.

4.3.7 Adding EVCSs

To verify whether the microgrid can meet the demand of EVCSs and to investigate the impact of introducing them, costs and constraints regarding EVCSs are considered in the asset sizing problem. The case study is run based on Case V. The annual load of a EVCS [32] is added into the existing electrical load. The results show that the designed microgrid can meet the demand of development of EVCSs in the community.

The EVCS data with a maximum of 226 kW is presented in Section 3.3. To validate whether the system can withstand challenges brought by EVCSs, the case study is done based on Case V. The charging demand for EVCSs is added into the original electrical demand, and the results are shown in Table 4.12 and 4.13.

Table 4.12: Rating of Each Resource Adding EVCSs

Energy Type	D(kW)	ESS(kWh)	CHP(kW)	Wind(kW)	PV(kW)	DR(kW)
Rating	965	0	1094	1000	415	220
Changes From Case V	+7.88%	-100%	+7.87%	0	0	0

Table 4.13: Investment and Operation Costs adding EVCSs

Total Cost/$MM	15.475	Change From Case V	+1.86%
Investment Cost/$MM	13.987	Change From Case V	+2.01%
Annual Operation Cost/$MM	1.489	Change From Case V	+0.38%

It is shown that the EVCS can be integrated into the existing community microgrid without resulting in too much increase in the costs. However, the increase of diesel and CHP generation is relatively large in comparison to Case V, which means a lot more fuels are consumed to feed electric cars. Also, no ESS is used in this case. In this sense, this is not the a desirable situation, although the costs do not change much. To reduce the amount of fuel consumption, the microgrid planner has to compromise between the wind and PV capacities and total costs, so that more wind and PV can be installed to substitute fuel energies.

4.4 Sensitivity Analysis

4.4.1 Overview of Sensitivity Analysis

Sensitivity analysis is an approach widely used in engineering to investigate how uncertainty in various inputs affects outputs. The results of a sensitivity analysis can be useful in many ways. First, robustness of the designed model can be validated when there is uncertainty in the inputs. The unknown relationship between the input and output can also be investigated. Furthermore, the inputs which do not have an influence on the output can be found and the model can be simplified, and the inputs which can bring big uncertainty to the output can be noticed so that the model can be modified for robustness. Besides, sensitivity analysis can be useful in finding optimization points, in Monte Carlo filtering, and in pre-selecting during the process of calibrating models [45].

To choose an appropriate sensitivity analysis approach, the problem restrictions must be considered first, including the computational expense, correlation of inputs, nonlinearity of models, model interaction and correlation between outputs. The computational cost needs to be considered when the single run time is long or when there are too many inputs. When the model is too large, emulators can be used, and screening method can be used when the dimensionality needs to be reduced. Variance-based measures are suitable to solve model response of nonlinear relationship with inputs. And sometimes multiple inputs can only cause significant variances together, and then the total-order sensitivity index can be used to capture such interactions. When the multiple outputs correlate with each other, the sensitivity analysis is harder to be done. In this thesis, the sensitivity analysis is simple because there is only one output, i.e. the net present value (NPV) cost of the asset sizing, which is equal to the total cost in value. Besides, the computational cost is not high.

The most commonly used approach to do sensitivity analysis is the one-at-a-time (OAT) test, in which only one factor is tuned in inputs to see how outputs would change. Although the OAT approach cannot show interactions between the investigated inputs, this thesis would still use this method because the focus is just to see which parameters can make the most and least influence on the results, as well as to validate that the proposed asset sizing approach is robust when the parameters change. The sensitivity analysis is done adding variations to the chosen parameters, and then variations in the output can be obtained. In [46], the load profile is modified and the effect to battery sizing is investigated. The load profile is scaled to be ten percent higher and lower as original data and then the peak is limited to 4 kW. In [47], a sensitivity analysis is done with a full factorial design of experiments [48] to find the most influential parameter for the yearly sizing and operation costs. Reference [49] did the sensitivity analysis to investigate robustness of the economic evaluations. The sensitivity analysis shows the effect of various parameters to the investment decisions.

In [50], the chosen parameters are PV generation capital cost, wind power capital cost, electricity price, interest rate, etc. For the case studied in [50], the most influential parameter is the wind capital cost given the system design of 3.6 MW of wind installation and 0.1 MW of PV installation. Another notable observation in [50] is that the electricity price does not affect the results greatly, which means profitability of the generation installation is not influenced by fluctuation of the electricity price. And the interest rate also has an influence on the results. When the interest rate is increased, more money value discount in the future would be brought in, so that the NPV would decrease.

4.4.2 Implementation of the Sensitivity Analysis

Based on the analysis above, the sensitivity analysis method in [50] is used in this thesis. The parameters involved and the results are shown in Table 4.14.

From the sensitivity analysis results, it is shown that the most influential parameter with a $\pm 10\%$ change is the wind generation capital cost. This is reasonable because the rating of wind generation is the biggest among all the resources. The PV capital cost also changes a lot because the PV capital cost is the biggest among the capital costs.

Table 4.14: Sensitivity Analysis

NPV change(%) \ variable change / Variable	+10%	-10%	+3%	-3%
Diesel Capital Cost	+1.68	-1.68	+0.50	-0.50
CHP Capital Cost	+2.07	-2.08	+0.62	-0.62
PV Capital Cost	+2.07	-2.07	+0.71	-0.71
Wind Capital Cost	+3.76	-3.76	+0.40	-0.40
ESS Capital Cost	+2.40	-2.40	+0.02	-0.02
ζ electric to heat ratio of CHP unit	+0.10	-0.10	+0.03	-0.03
v power to energy ratio of the ESS	-0.09	+0.09	-0.03	+0.02

Two important parameters not included in the table are C_{gas} and C_{die}. It is because the two parameters do not affect the NPV cost with the extent of $\pm 10\%$ or $\pm 3\%$. It is until the parameter C_{gas} increases by three times its original value that the NPV would increase by 2.55%, and the NPV increases by 0.47% when C_{die} increases by 50 times. This is because the amount of diesel and gas used in this case study is low. If there are more diesel or gas generators in the microgrid, or the diesel and gas prices are higher, the system would be more sensitive to the change of the price of the fuels.

The electricity to heat ratio of CHP units, ζ, and the power to energy ratio of the energy storage resource, v, also have some influence on the NPV cost. Increasing ζ would require more electricity to produce the same amount of heat as before, thus increasing the NPV of the total cost. But if the parameter v is increased, less strict constraints would be applied to the ESS charging power. Further research can be done to investigate the influence made by other parameters related to the resources.

4.5 Chapter Summary

In this chapter, the objective and constraints of the asset sizing problem are proposed and case studies are done. Diesel generators, wind generation and ESSs are considered in the baseline case. PV generation, CHP units and demand response are added later to discuss the impacts of the components to the microgrid. In Case VI, the main grid is connected to the microgrid with the form of a flat power profile. An EVCS is also added as a significant electrical load. Finally, the sensitivity analysis is done based on Case V. The results obtained in this chapter are used as inputs for the economic dispatch problem discussed in the next chapter.

Chapter 5

Implementing Community Microgrid Economic Dispatch with a Decision-Tree-Based EMS

5.1 Overview

In conventional economic dispatch (ED) problems, there are many methods including the equal incremental cost method, dynamic programing, linear programming, the Ford-Fulkerson method, evolutionary programming, the genetic algorithm, etc. [51]. Among the many methods, linear programming is widely used because it is fast and reliable and is capable to handle many constraints related to time and security requirements. In traditional ways to do economic dispatch, the objective is to minimize operational costs, including maintenance costs as is presented in Chapter 2. In [51], PV generation, wind generation, diesel generators and CHP units are considered in dispatching, and the objective is to minimize operational costs and pollution. Other ED algorithms may also consider grid losses. In the electricity market environment, the objective function can be chosen as minimizing electricity purchasing costs of the whole grid rather than generation costs. The constraints in ED are also subject to change. Apart from power balance and generator capacity constraints, security constraints are also considered in some papers. In this thesis, constraints for the economic dispatch problem are the same as in the asset sizing problem, but capacities of generators are regarded as parameters rather than variables in the sizing stage. Capacities are generated as outputs of the sizing problem.

Economic dispatch problems can also be solved with machine learning approaches, which do not focus on optimization formulations but on large amounts of training data. Data mining methods, involving methods of machine learning and statistics, can be effective in the analysis of large-scale electricity models. Reference [52] proposes an economic dispatch algorithm with Back Propagation Neural Network (BPNN) and Radial Basis Function Neural Network (RBFNN). The input is the electricity demand and the output is an optimal real power dispatch, which is obtained with evolutional programming. The main benefit of the proposed method is that it is less time consuming for online estimation.

Among the machine learning approaches, a decision tree algorithm is widely used for its low computational burden and learnt principles for further interpretation, as well as the capability of managing uncertainties in power systems [53]. Applications of DT in power systems involve security assessment, preventive and corrective control, protection, fault diagnosis and etc. Reference [54] shows the possibility to solve optimization problems in economic dispatch with DT algorithm taking environmental constraints into consideration. Reference [54] is an improvement of [55], in which numerical convergence can be improved. In [56], fuzzy logic is added so that the generating costs are reduced, and more uncertainties can be considered in the load.

Reference [57] develops a decision tree based on state-of-charge and power-limiting dispatch rules. The structure of the decision tree is pre-defined by constraints rather than learnt from training data. Renewable generation is consumed first and diesel generators serve as back-up generation only when the minimum threshold of battery state of charge (SoC) is reached. In this thesis, a decision tree to do the economic dispatch is trained with machine learning approaches.

In this chapter, a decision-tree-based energy management system (EMS) for economic dispatch is proposed. The EMS is tested on the same community microgrid as is in Chapter 4 and can be implemented in an industrial controller in the future work. A decision tree is ideal for a community microgrid, because all of the assets in Chapter 2 are controlled generally through programmable logic controllers (PLCs), whose programming language (ladder logic) is effectively the implementation of a decision tree.

5.2 Decision-Tree-Based EMS Data Analysis

The optimal asset sizes of the microgrid asset sizing problem are passed down to the economic dispatch problem as inputs. A total of 8760 data points in a year are divided as training set, validation set and test set.

The input data of economic dispatch at time t includes its corresponding PV and wind generation, electric load and battery SoC of the former time point, $(t-1)$. The actual input related to renewable generation could also be the weather prediction of the future time point, which can be converted into renewable energy generation by certain probability distribution functions. However, PV and wind generation data are taken as inputs directly, since this thesis does not focus on the transforming relationships between weather and generator outputs.

All the components discussed in this thesis are included. There are four parameters in the input data: L_{enet}, L_h, E_{es}, and E_r^e. Parameter L_{enet} is the net electricity load, which is equal to the total electricity load L_e minus wind and PV generation. Parameter L_h represents thermal load. Parameters E_{es} and E_r^e are the SoC of ESSs and energy reduced by demand response, respectively. It should be noticed that E_{es} and E_r^e are actually $E_{es}(t-1)$ and $E_r^e(t-1)$, which correspond to the energy at the beginning rather than the end of time point t.

The output data includes power generation levels of diesel generators, CHP units and batteries, as well as power involved in demand response. Generators corresponding to the outputs are dispatchable and are decided by electric load and renewable generation. To meet the power balance constraints, three of the outputs with the highest accuracy are generated by the decision tree and the remaining one is then calculated with power balance equations.

5.3 Decision Tree Algorithm Outline

Decision trees are a type of supervised machine learning algorithm [53]. The flowchart-like structures of decision trees, involving features and decision rules, are easy to interpret. There are no assumptions regarding probability distributions needed in setting up and training decision tree algorithms. Both classification and regression problems can be solved with decision tree methods, and in this thesis a decision tree regressor is conducted.

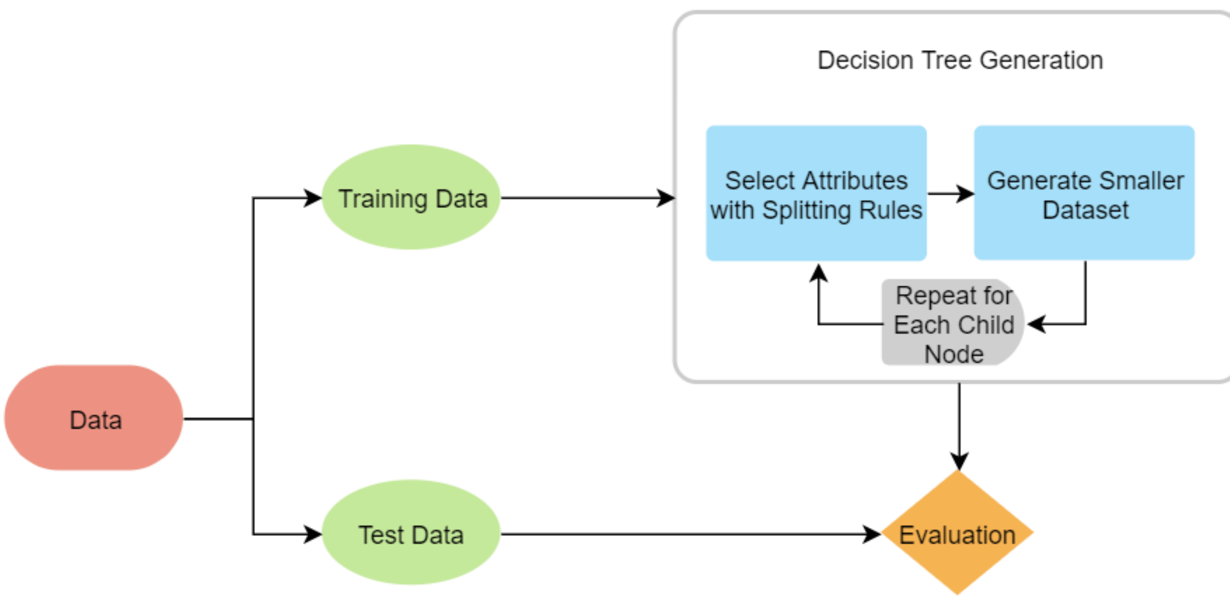

Figure 5.1: Generation of a Decision Tree.

In the implementation of a decision tree, the best attribute is selected first with a proper splitting rule. The chosen attribute is set as a decision node which can break a dataset into subsets. The above process is repeated on each child node until all the tuples are categorized into the same attribute value or no more remaining attributes or instances are left, as is shown in Figure 5.1 [58]. As for splitting rules, the most common measures for classification problems are Information Gain, Gain Ratio and Gini Index. For regression problems, popular rules are Mean Squared Error (MSE) and Mean Absolute Error. In this thesis, MSE is proven to be the best criterion. The formulation of MSE is shown in (5.1).

$$\begin{aligned} \bar{y}_m &= \tfrac{1}{N_m} \sum_{i \in N_m} y_i \\ MSE &= \tfrac{1}{N_m} \sum_{i \in N_m} (y_i - \bar{y}_m)^2 \end{aligned} \tag{5.1}$$

in which y_i is the observed value of the variable to be predicted, i is the variable numbering, $\bar{y}_m$ is the average value, and N_m is the total number of data points.

When there is a correlation between the outputs, independent models of the outputs may not guarantee the highest accuracy. In a decision tree regressor, the output can be set as arrays which represent multiple correlated outputs, and the prediction can be done simultaneously within one model. The training time would be decreased, and the overall accuracy of outputs is often boosted. There would be changes in the structure of the corresponding decision tree. Multiple outputs would be stored in leaves, and the splitting criteria would become the average reduction of all the several outputs rather than reduction of just one output.

In this thesis, several outputs are first generated independently using the grid search approach to tune the best parameters. The multi-output approach is then used to find a method with the highest overall accuracy. In the grid search approach, a fit-and-score method [59] is used and an exhaustive search over the most important parameters is done. Cross-validation is also used in this approach.

5.4 Decision Tree Design and Calculation

5.4.1 Training and Pruning of Decision Trees

The decision-tree-based EMS is illustrated on a case study in this section. Outputs of case in Section 4.3.7 in the asset sizing problem with EVCSs integrated are taken as input data in the economic dispatch problem. Parameters of the decision tree regressor are chosen by the method of GridSearchCV [59]. The training and testing data is the first year data from the asset sizing results. For the first step, single outputs are generated separately, and output of the diesel generators, P_{ed}, is taken as an example in this section. The accuracy score reaches 97.26%. Implementation of the other three outputs are similar.

The topology of the decision tree could be visualized but is too large. With the same depth of six layers, pruning produces less leaf nodes and helps with overfitting and not being able to generalize to unseen inputs. Although the results of the validation set show that the decision tree is not overfitted, and the tree is prevented from overfitting by parameters like the minimum number of samples required to be at a leaf node and the maximum depth of the tree, post-pruning is applied with the cost complexity pruning approach to make the topology simpler and to improve robustness of the decision tree [60].

Figures 5.2 and 5.3 show how the total impurity (a measure of the homogeneity of the labels at the node [61]), number of nodes and depth of the tree vary when $alpha$, the cost complexity parameter (a parameter to control the size of the decision tree and to select the optimal tree size [61]), increases. The higher the value of $alpha$ is, the more nodes are pruned in the decision tree, and there would be fewer nodes and a shallower depth.

To choose an appropriate $alpha$ value, the mean squared error (MSE) of each validation set is calculated. When the value of $alpha$ is 18, the MSE of the validation set is not too low compared with the accuracy before the tree is pruned. The MSE is 96.59% then, and is slightly lower than the score before pruning but the structure of the decision tree is a lot simpler, as is shown in Figure 5.4.

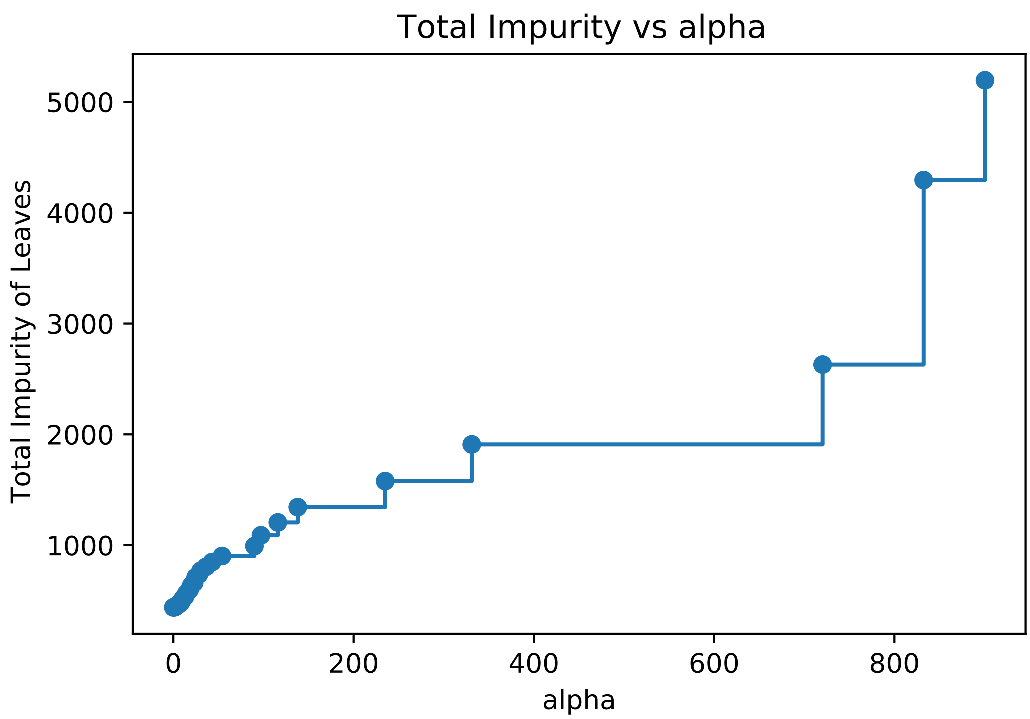

Figure 5.2: Total Impurity Versus $alpha$.

Comparison of the former decision tree and the pruned tree setting the $alpha$ value at 18 are shown in Figure 5.5 and 5.6. The decision tree can be more robust and less likely to be overfitted with a greatly simplified topology by a minor reduction of the accuracy score of 0.67% with the test set. Also, the annual running costs are 1.168 times the optimized result by GAMS/CPLEX due to regression tree errors. This is analyzed in detain in Section 5.5.

5.4.2 Improving the Results with a Multi-Output Decision Tree

Results for all the single outputs are listed in Table 5.1, from which three of them would be chosen and the remaining one would be generated based on power balance relationships. As can be seen, outputs of diesel generators and CHP generators can be two of the desirable outputs, but neither of scores of the power of ESS or the main grid is high. This problem could be addressed with a multi-output decision tree.

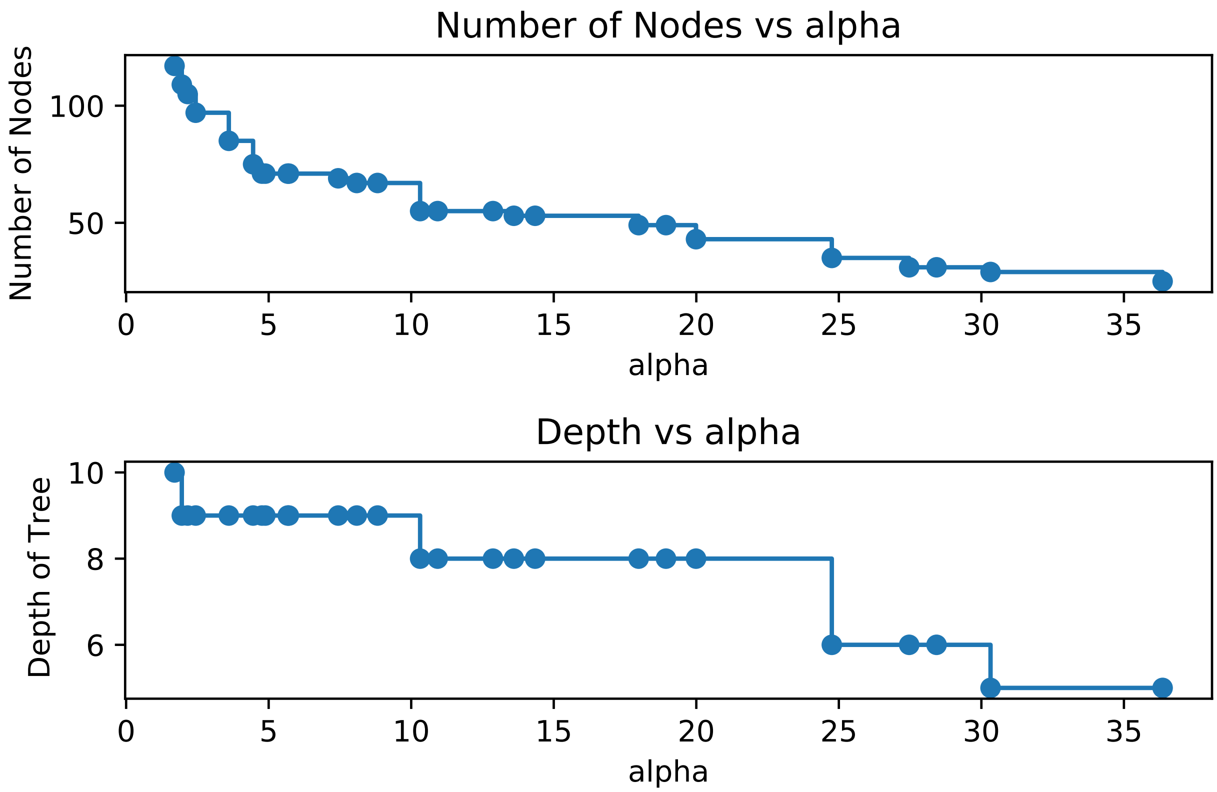

Figure 5.3: Number of Nodes and Depth Versus $alpha$.

First, three of the outputs with the highest scores are taken as a whole in the multi-output decision tree model, and the MSE of the test set reaches 85.17%. Also, a better option is found that the power generation of the ESS and diesel generators can be predicted together scoring 94.49%, and generation of CHP units are calculated separately, scoring 84.76%. The electric power from the main grid reaches an accuracy of 75.20%. This is the best way in this case study to do economic dispatch for this typical community microgrid, and the topology of the decision tree is shown in Figure 5.7. For different case studies, it may depend on the choice of single or multi output decision tree and combinations of multi outputs.

It should be noticed that how the decisions are achieved can be clearly seen in the structure of the decision trees shown in Figures 5.5-5.7. The parameters x_0, x_1, x_2 and x_3 correspond to the inputs L_{enet}, L_h, E_{es} and E_r^e introduced in Section 5.2, respectively. For

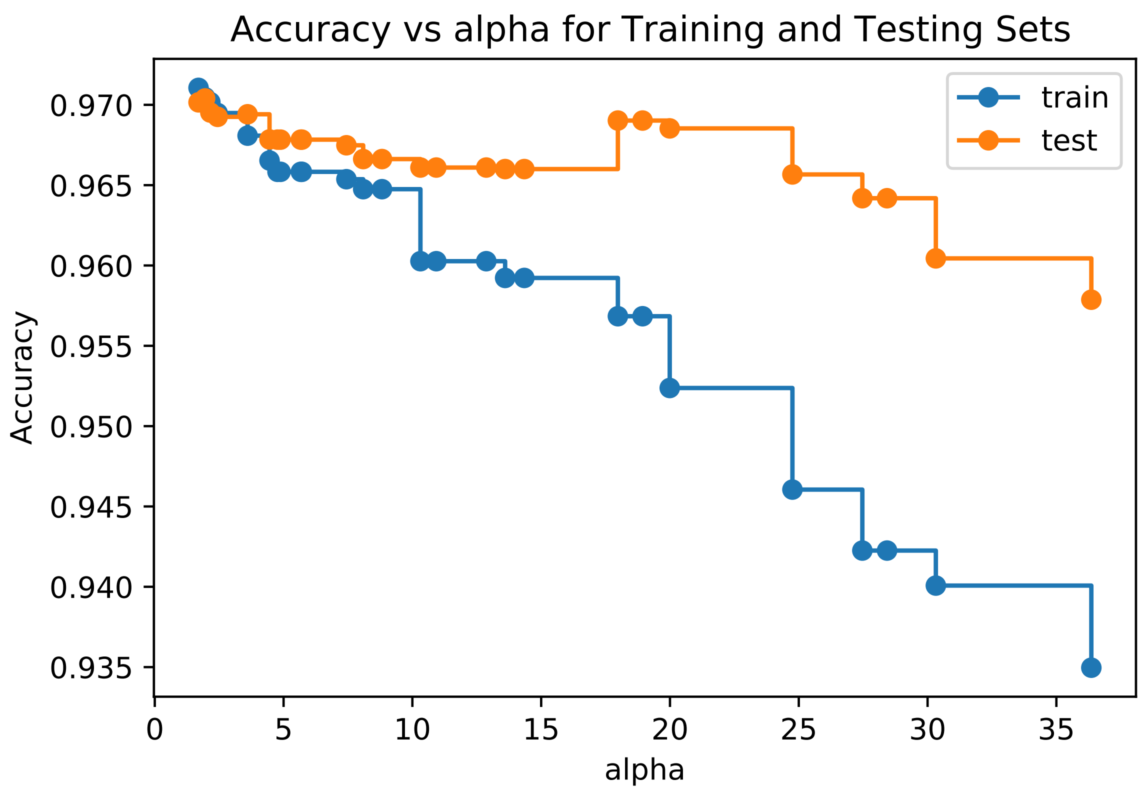

Figure 5.4: Accuracy Versus $alpha$.

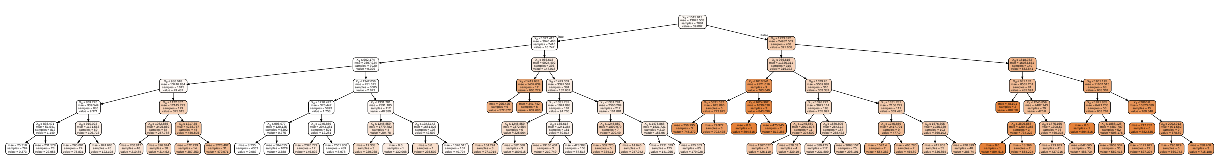

Figure 5.5: Decision Tree Before Pruning.

example, in the root node of Figure 5.7, the splitting criteria $X_0 \leq 535.371$ means whether the net load is less or equal to 535.571 kW. It is also a benefit of decision trees that they are very interpretable.

Table 5.1: MSE Score of Single Outputs

Power Output	Energy Storage	Diesel	CHP	Main Grid
MSE Score	26.41%	97.26%	83.51%	45.62%

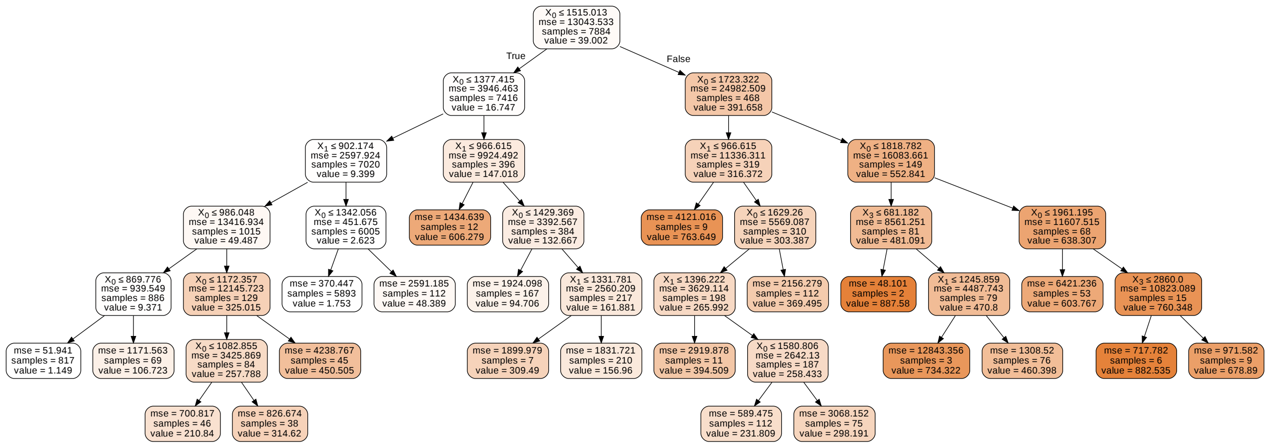

Figure 5.6: Decision Tree After Pruning.

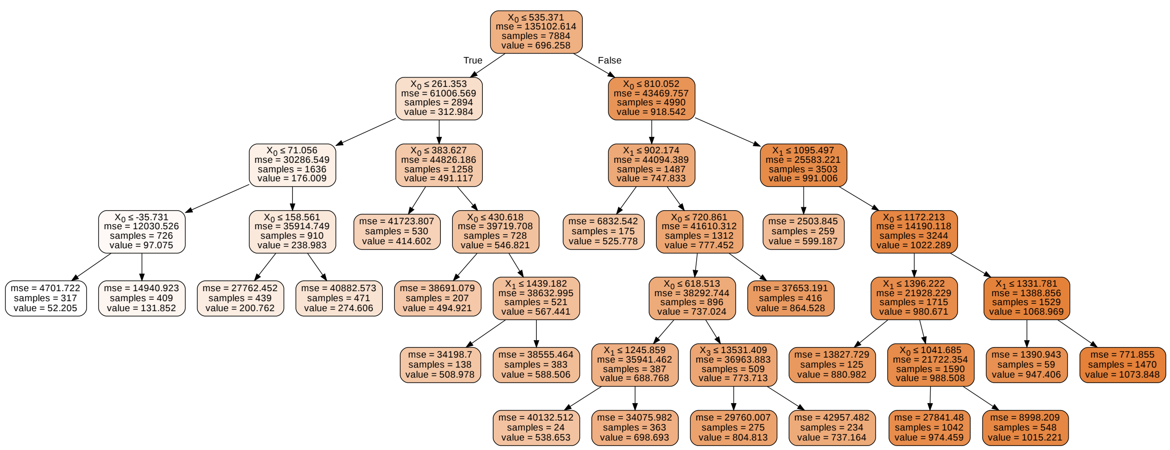

Figure 5.7: Multi-output Decision Tree for Energy Storage and Diesel Generation.

5.5 Evaluation of the Decision-Tree-Based EMS Against Fully-Optimized Economic Dispatch

The decision-tree-based economic dispatch is designed to decrease the calculation time so as to be implemented in an industrial controller. In the real time simulation of power systems, simulators are required to solve model calculations within each time step, which is the same as the real-world clock [62]. Simulations would be real time only if the execution time of the simulation is within the chosen time step. On the contrary, if a calculation cannot be done within the set time step, system models must be simplified, or the time step has to be increased [63]. Otherwise, the simulation would be offline.

In traditional power grids, it is assumed that generation is feasible for dispatch and generation schedules do not change much. In real time economic dispatch, calculations are typically done every five minutes at the nodal level [64]. Also, calculations need to be done when the status of a generator or a tie line changes. Although the calculation speed of traditional economic dispatch algorithms has been effective so far for conventional power grids, faster economic dispatch calculations are needed in microgrid circumstances [64]. With the high penetration of renewable energies in many microgrid scenarios like the ones studied in this thesis, a significant portion of conventional controllable generators are replaced by intermittent renewable generation, and forecast errors require more frequent changes in dispatchable generation setpoints. Therefore, more frequently updated generation controls are required and the computational speed in real-time operations is critical to deal with challenges brought up by renewable energy resources. Besides, disturbances are increased with penetration of renewable energies, so faster algorithms are required to integrate ramp-rate capability calculations in the future work [64].

To address these issues mentioned above, a decision-tree-based EMS is used in economic dispatch to shorten the calculation time at the cost of optimality to an acceptable degree. The fully-optimized optimization approach is done (which was used to train the DTs) with the same constraints as is in the sizing problem, but just capacities of generation are set as parameters rather than variables and the objective becomes the minimization of operational costs. The runtime for an entire year is 105.53 seconds and the average calculation time for a single time step is 12.04 ms. The operating environment is a PC with Intel (R) Core (TM) i7-6700HQ CPU @ 2.6 GHz 3.5 GHz (8.00 GB RAM) and the operating system is Windows 10. However, once the decision tree is trained, the average runtime of the decision tree to do the forecast is 1.056 ms for a single time step. At the same time, the annual operational cost related to the decision tree is 1.168 times of the optimized result.

The price paid for the great reduction of calculation time is the increase of the operational cost, and this can be improved further in future work.

5.6 Chapter Summary

In this chapter, a literature review on different economic dispatch algorithms is done, and a decision-tree-based EMS is introduced in detail. The decision tree is trained and tested, and pruned to prevent overfitting and simplify the topology. A multi-output decision tree is also used to improve the results. As a comparison, a traditional optimization method is used in the economic dispatch to evaluate the decision tree algorithm in time and operational costs. In the next chapter, recommendations for future work are proposed.

Chapter 6

Summary and Future Work

In this chapter, the work done in this thesis is summarized, and recommendations for future work are brought up.

6.1 Summary

In this thesis, community microgrids and typical components are modeled to explore asset sizing and economic dispatch problems. A decision-tree-based EMS is used in the economic dispatch problem to account for realistic in-field control hardware which typically consists of programmable logic controllers. Components such as CHP units, energy storage systems and electric vehicle charging stations, which are largely located in microgrids these years, are integrated and their impacts are investigated with several case studies.

Community microgrid components are modeled as dispatchable or non-dispatchable units. The non-dispatchable units are regarded as input data later in the EMS when doing the economic dispatch, and the dispatchable units are taken as outputs. Distributed generation, energy storage systems and demand response are all modeled in this thesis. Important parameters related to CHP units, ESSs and other components are listed. The steady state description of ESSs and electrical and thermal demand response formulations are used in asset sizing. As an important part of the electrical load, electric vehicle charging stations are modeled and EV charging behaviors are studied. EVCS charging and discharging are then integrated into the load to validate whether community microgrids can withstand such significant fluctuations and high peaks.

In the asset sizing problem, the objective is to minimize the total annual costs including investment and a representation of future operational costs. Constraints related to each component are also taken into account. A typical set of demand data is clustered into three distinct clusters, but there is no such clear pattern for a combined Demand-Wind-PV dataset. Therefore, the hourly data in a year rather than the clustered data are taken as inputs of the sizing problem. Case studies are done concerning different components of a typical microgrid. ESSs are found to be necessary when there are intermittent energy resources. Wind and PV generation, as well as CHP units, can reduce the costs in the long run. When demand response is added, the ESS rating decreases largely, and the total cost also decreases. Lastly, an EVCS is integrated, and the results show that the costs does not increase too much. Taking Case V developed in Chapter 4 as an example, a sensitivity analysis is done, and the parameters which may have an influence on the net present value costs are investigated. The results of the sensitivity analysis can be used in the design and upgrade of microgrids.

A decision tree regressor method is used in the economic dispatch problem. With the nature of low computational burden and desirable interpretability, the decision tree algorithm is chosen from many machine learning approaches to approximate computation-heavy optimization-based algorithms. The structure of the decision tree is trained from data generated in the sizing stage. The grid search approach is used in choosing the best parameters. To prevent overfitting and to improve robustness of the decision tree, a post-pruning method is applied. Since the accuracy of some results are not desirable, a multi-output decision tree is developed and the overall results improve significantly. An optimization method is also used to compare with the decision-tree-based EMS, and the results show that the decision tree algorithm can decrease the runtime at the cost of optimality with an acceptable increase of operational costs.

6.2 Recommendations for Future Work

In this thesis, community microgrid asset sizing and economic dispatch problems are addressed with the proposed optimal sizing and decision tree approaches. Case studies are done considering diesel generators, wind and PV generation, energy storage systems, CHP units and demand response. However, for community microgrids, new components and new techniques of existing parts can be introduced, and more detailed modeling of the problems can be developed. Besides, other research focuses based on the models and results can be developed. Some potential extensions of this thesis can be as follows:

1. Other types of energy resources could be integrated into microgrids. The case study used in this thesis can be easily extended with other renewable energy types, and technologies used in existing cases can be replaced. For example, flywheels can substitute the batteries in the energy storage system, and parameters of ESSs are also subject to change. The integration of different storage media require that decision time steps are commensurate with their typical time of action (e.g., in the case of flywheels, one has to have time steps in the five-ten minutes range).

2. The proposed asset sizing and economic dispatch approach can be applied to other kinds of microgrids such as military microgrids, institutional microgrids and remote village microgrids. These microgrids have different requirements. Military microgrids require quick deployment, institutional microgrids meet specific demand of the clients, and remote village microgrids are always under island mode [65]. For each kind of microgrids, the proposed sizing and economic dispatch approach can be applied and explored further.

3. More complicated demand response technologies can be included in the asset sizing problem. Many research works have been done to integrate DR into microgrids with

different models. Some approaches such as the price bidding strategy and occupancy-based DR introduced in [66] can be explored.

4. Dynamic charging/discharging rates can be applied in EVCSs. This would make the sizing problem nonlinear. Due to the high demand of power increase in fast charging, it is not always desired to charge at the highest rate. Many customers are willing to choose normal charging with lower prices when they can wait, especially in the charging stations in markets and work places where fast charging is not necessary. Some EVCSs can adjust the charging speed according to the expected waiting time. Both customers and microgrids may benefit from the dynamic charging/discharging rate.

5. More inputs can be included in the economic dispatch decision tree. There are only four parameters in the decision tree adopted in this thesis. If more data can be collected from generation stations, more detailed models can be used in the sizing problem and there can be more inputs for the decision tree.

6. Real time simulations can be done based on the proposed methods. Community microgrid models can be loaded into a real time simulator to do a hardware-in-the-loop test. Stability and flexibility can be discussed further.

Bibliography

[1] L. Orsini, S. Kessler, J. Wei, and H. Field, "How the brooklyn microgrid and transactive grid are paving the way to next-gen energy markets," in *The Energy Internet*, pp. 223–239, Elsevier, 2019.

[2] R. Stock, "Energy disparities and (under) development in sub-saharan africa," in *Handbook on the Geographies of Energy*, Edward Elgar Publishing, 2017.

[3] A. Jäger-Waldau, "Snapshot of photovoltaics-February 2018," *EPJ Photovoltaics*, vol. 9, p. 6, 2018.

[4] G.-G. W. E. Council, "Global wind report 2018, 2019," *URL: www. gwec. net.(Cited on page 5.)*, 2019.

[5] M. Hojo, "Distributed energy resources and power electronics," in *Integration of Distributed Energy Resources in Power Systems*, pp. 229–235, Elsevier, 2016.

[6] Y.-Y. Hong, W.-C. Chang, Y.-R. Chang, Y.-D. Lee, and D.-C. Ouyang, "Optimal sizing of renewable energy generations in a community microgrid using Markov model," *Energy*, vol. 135, pp. 68–74, 2017.

[7] GAMS Development Corporation, Washington, DC, USA, *GAMS - A User's Guide, GAMS Release 24.2.1*, 2013.

[8] IBM ILOG CPLEX Optimization Studio, *CPLEX User's Manual, Version 12 Release 8*, 2017.

[9] M. Quashie, *Optimal planning of advanced microgrids with an energy management system*. PhD thesis, McGill University Libraries, 2018.

[10] M. Liu, S. Wang, Y. Zhao, H. Tang, and J. Yan, "Heat–power decoupling technologies for coal-fired CHP plants: Operation flexibility and thermodynamic performance," *Energy*, vol. 188, p. 116074, 2019.

[11] M. Quashie, F. Bouffard, C. Marnay, R. Jassim, and G. Joós, "On bilevel planning of advanced microgrids," *International Journal of Electrical Power & Energy Systems*, vol. 96, pp. 422–431, 2018.

[12] L. B. Shi, Z. X. Weng, L. Z. Yao, and Y. X. Ni, "An analytical solution for wind farm power output," *IEEE Transactions on Power Systems*, vol. 29, no. 6, pp. 3122–3123, 2014.

[13] "The general pattern of wind speed variations." `http://xn--drmstrre-64ad.dk/wp-content/wind/miller/windpower%20web/en/tour/wres/weibull.htm`, Jan. 2020.

[14] E. Dupont, R. Koppelaar, and H. Jeanmart, "Global available wind energy with physical and energy return on investment constraints," *Applied Energy*, vol. 209, pp. 322–338, 2018.

[15] A. Feijóo and D. Villanueva, "Four-parameter models for wind farm power curves and power probability density functions," *IEEE Transactions on Sustainable Energy*, vol. 8, no. 4, pp. 1783–1784, 2017.

[16] H.-z. Wang, G.-q. Li, G.-b. Wang, J.-c. Peng, H. Jiang, and Y.-t. Liu, "Deep learning based ensemble approach for probabilistic wind power forecasting," *Applied energy*, vol. 188, pp. 56–70, 2017.

[17] Alhazmi, Yassir, "Planning model for implementing electric vehicle charging infrastructure in distribution system." UWSpace, 2016. `http://hdl.handle.net/10012/10766`.

[18] G. Wang, Z. Xu, F. Wen, and K. P. Wong, "Traffic-constrained multiobjective planning of electric-vehicle charging stations," *IEEE Transactions on Power Delivery*, vol. 28, no. 4, pp. 2363–2372, 2013.

[19] H. Cai, X. Jia, A. S. Chiu, X. Hu, and M. Xu, "Siting public electric vehicle charging stations in beijing using big-data informed travel patterns of the taxi fleet," *Transportation Research Part D: Transport and Environment*, vol. 33, pp. 39–46, 2014.

[20] A. Ip, S. Fong, and E. Liu, "Optimization for allocating bev recharging stations in urban areas by using hierarchical clustering," in *2010 6th International conference on advanced information management and service (IMS)*, pp. 460–465, IEEE, 2010.

[21] F. He, D. Wu, Y. Yin, and Y. Guan, "Optimal deployment of public charging stations for plug-in hybrid electric vehicles," *Transportation Research Part B: Methodological*, vol. 47, pp. 87–101, 2013.

[22] W. Yao, J. Zhao, F. Wen, Z. Dong, Y. Xue, Y. Xu, and K. Meng, "A multi-objective collaborative planning strategy for integrated power distribution and electric vehicle charging systems," *IEEE Transactions on Power Systems*, vol. 29, no. 4, pp. 1811–1821, 2014.

[23] W. Yao, J. Zhao, F. Wen, Y. Xue, and G. Ledwich, "A hierarchical decomposition approach for coordinated dispatch of plug-in electric vehicles," *IEEE Transactions on Power Systems*, vol. 28, no. 3, pp. 2768–2778, 2013.

[24] Z.-f. Liu, W. Zhang, X. Ji, and K. Li, "Optimal planning of charging station for electric vehicle based on particle swarm optimization," in *IEEE PES Innovative Smart Grid Technologies*, pp. 1–5, IEEE, 2012.

[25] A. Y. Lam, Y.-W. Leung, and X. Chu, "Electric vehicle charging station placement," in *2013 IEEE International Conference on Smart Grid Communications (SmartGridComm)*, pp. 510–515, IEEE, 2013.

[26] T. D. Chen, K. M. Kockelman, and M. Khan, "Locating electric vehicle charging stations: Parking-based assignment method for Seattle, Washington," *Transportation research record*, vol. 2385, no. 1, pp. 28–36, 2013.

[27] Z. Liu, F. Wen, and G. Ledwich, "Optimal siting and sizing of distributed generators in distribution systems considering uncertainties," *IEEE Transactions on power delivery*, vol. 26, no. 4, pp. 2541–2551, 2011.

[28] S. Ge, L. Feng, and H. Liu, "The planning of electric vehicle charging station based on grid partition method," in *2011 International Conference on Electrical and Control Engineering*, pp. 2726–2730, IEEE, 2011.

[29] J.-h. Liu and Z. Ke, "The influence of ev dynamic charging power on microgrid and the optimal control method," in *2019 International Conference on Advanced Mechatronic Systems (ICAMechS)*, pp. 278–283, IEEE, 2019.

[30] `https://www.fleetcarma.com/`. Accessed December 5, 2019.

[31] Y. Zhou, Z. Li, and X. Wu, "The multiobjective based large-scale electric vehicle charging behaviours analysis," *Complexity*, vol. 2018, 2018.

[32] M. Anand, B. Bagen, and A. Rajapakse, "Probabilistic reliability evaluation of distribution systems considering the spatial and temporal distribution of electric vehicles," *International Journal of Electrical Power & Energy Systems*, vol. 117, p. 105609, 2020.

[33] A.-L. Barabasi, "The origin of bursts and heavy tails in human dynamics," *Nature*, vol. 435, no. 7039, pp. 207–211, 2005.

[34] D. S. Kirschen, J. Ma, V. Silva, and R. Belhomme, "Optimizing the flexibility of a portfolio of generating plants to deal with wind generation," in *2011 IEEE power and energy society general meeting*, pp. 1–7, IEEE, 2011.

[35] U. Akram, M. Khalid, and S. Shafiq, "Optimal sizing of a wind/solar/battery hybrid grid-connected microgrid system," *IET Renewable Power Generation*, vol. 12, no. 1, pp. 72–80, 2017.

[36] "K-means clustering." `https://scikit-learn.org/stable/modules/generated/sklearn.cluster.KMeans.html`, Jan. 2020.

[37] "Elbow method." `https://www.scikit-yb.org/en/latest/api/cluster/elbow.html`, Jan. 2020.

[38] "Selecting the number of clusters with silhouette analysis on kmeans clustering." `https://scikit-learn.org/stable/auto_examples/cluster/plot_kmeans_silhouette_analysis.html`, Jan. 2020.

[39] S. Y. Lee, Y. G. Jin, and Y. T. Yoon, "Determining the optimal reserve capacity in a microgrid with islanded operation," *IEEE Transactions on Power Systems*, vol. 31, no. 2, pp. 1369–1376, 2015.

[40] A. H. Habib, V. R. Disfani, J. Kleissl, and R. A. de Callafon, "Optimal energy storage sizing and residential load scheduling to improve reliability in islanded operation of distribution grids," in *2017 American Control Conference (ACC)*, pp. 3974–3979, IEEE, 2017.

[41] Y. Luo, L. Shi, and G. Tu, "Optimal sizing and control strategy of isolated grid with wind power and energy storage system," *Energy Conversion and Management*, vol. 80, pp. 407–415, 2014.

[42] A. Golder, J. Jneid, J. Zhao, and F. Bouffard, "Machine learning-based demand and pv power forecasts," in *2019 IEEE Electrical Power and Energy Conference (EPEC)*, pp. 1–6, IEEE, 2019.

[43] F. D. Santillán-Lemus, H. Minor-Popocatl, O. Aguilar-Mejía, and R. Tapia-Olvera, "Optimal economic dispatch in microgrids with renewable energy sources," *Energies*, vol. 12, no. 1, p. 181, 2019.

[44] `http://dkasolarcentre.com.au/locations`. Accessed April 16, 2018.

[45] E. Fabrizio and V. Monetti, "Methodologies and advancements in the calibration of building energy models," *Energies*, vol. 8, no. 4, pp. 2548–2574, 2015.

[46] M. Hunt and A. Benigni, "Sensitivity analysis of optimal battery sizing to differences in microgrid use," in *2019 International Conference on Clean Electrical Power (ICCEP)*, pp. 444–449, IEEE, 2019.

[47] R. Rigo-Mariani, B. Sareni, and X. Roboam, "Fast power flow scheduling and sensitivity analysis for sizing a microgrid with storage," *Mathematics and Computers in Simulation*, vol. 131, pp. 114–127, 2017.

[48] M. A. S. N. Junior, T. C. de Oliveira, J. M. de Carvalho Filho, and J. P. G. de Abreu, "Design of experiments for sensitivity analysis of voltage sags variables," in *2012 IEEE 15th International Conference on Harmonics and Quality of Power*, pp. 398–402, IEEE, 2012.

[49] C. W. Tan, T. C. Green, and C. A. Hernandez-Aramburo, "A stochastic method for battery sizing with uninterruptible-power and demand shift capabilities in pv (photovoltaic) systems," *Energy*, vol. 35, no. 12, pp. 5082–5092, 2010.

[50] A. González, J.-R. Riba, A. Rius, and R. Puig, "Optimal sizing of a hybrid grid-connected photovoltaic and wind power system," *Applied Energy*, vol. 154, pp. 752–762, 2015.

[51] A. Ghods, F. Al Farid, S. Barman, E. Sheikhi, and U. Salma, "Optimizing economical dispatch of a microgrid in islanding mode," in *8th International Conference on Electrical and Computer Engineering*, pp. 297–300, IEEE, 2014.

[52] M. A. Babu, R. Mahalakshmi, S. Kannan, M. Karuppasamypandiyan, and A. Bhuvanesh, "On-line economic dispatch of distributed generation using artificial neural networks," in *International Conference on Swarm, Evolutionary, and Memetic Computing*, pp. 275–283, Springer, 2014.

[53] C. Liu, Z. H. Rather, Z. Chen, and C. L. Bak, "An overview of decision tree applied to power systems," *International Journal of Smart Grid and Clean Energy*, vol. 2, no. 3, pp. 413–419, 2013.

[54] C. Roa-Sepulveda, "Environmental economic dispatch via decision trees," in *The 1996 31 st Universities Power Engineering Conference. Part 1(of 3)*, pp. 310–313, 1996.

[55] C. Roa-Sepulveda and M. Herrera, "A solution to the economic dispatch problem using decision trees," *Electric Power Systems Research*, vol. 56, no. 3, pp. 255–259, 2000.

[56] C. Roa-Sepulveda, M. Herrera, B. Pavez-Lazo, U. Knight, and A. Coonick, "Economic dispatch using fuzzy decision trees," *Electric Power Systems Research*, vol. 66, no. 2, pp. 115–122, 2003.

[57] C. Sun, J. N. Paquin, F. Al Jajeh, G. Joos, and F. Bouffard, "Implementation and CHIL testing of a microgrid control system," in *2018 IEEE Energy Conversion Congress and Exposition (ECCE)*, pp. 2073–2080, IEEE, 2018.

[58] "Generation of a decision tree." `https://medium.com/pursuitnotes/day-16-decision-tree-classification-2-db7d7d224f4`, Jan. 2020.

[59] "sklearn.model_selection.gridsearchcv." `https://scikit-learn.org/stable/modules/generated/sklearn.model_selection.GridSearchCV.html`, Feb. 2020.

[60] G. H. John, "Robust decision trees: Removing outliers from databases.," in *KDD*, vol. 95, pp. 174–179, 1995.

[61] "sklearn.tree.decisiontreeregressor." `https://scikit-learn.org/stable/modules/generated/sklearn.tree.DecisionTreeRegressor.html`, Feb. 2020.

[62] N. Yorino, H. M. Hafiz, Y. Sasaki, and Y. Zoka, "High-speed real-time dynamic economic load dispatch," *IEEE transactions on power systems*, vol. 27, no. 2, pp. 621–630, 2011.

[63] M. O. Faruque, T. Strasser, G. Lauss, V. Jalili-Marandi, P. Forsyth, C. Dufour, V. Dinavahi, A. Monti, P. Kotsampopoulos, J. A. Martinez, *et al.*, "Real-time simulation technologies for power systems design, testing, and analysis," *IEEE Power and Energy Technology Systems Journal*, vol. 2, no. 2, pp. 63–73, 2015.

[64] Y. Sasaki, T. Tsurumi, N. Yorino, Y. Zoka, and A. Beni Rehiara, "Real-time dynamic economic load dispatch integrated with renewable energy curtailment," *Journal of International Council on Electrical Engineering*, vol. 9, no. 1, pp. 85–92, 2019.

[65] D. T. Ton and M. A. Smith, "The US Department of Energy's microgrid initiative," *The Electricity Journal*, vol. 25, no. 8, pp. 84–94, 2012.

[66] C. D. Korkas, S. Baldi, I. Michailidis, and E. B. Kosmatopoulos, "Occupancy-based demand response and thermal comfort optimization in microgrids with renewable energy sources and energy storage," *Applied Energy*, vol. 163, pp. 93–104, 2016.